Eur. Phys. J. C (2015) 75:237
DOI 10.1140/epjc/s10052-015-3435-4

THE EUROPEAN PHYSICAL JOURNAL C

Regular Article - Experimental Physics

Nuclear effects on the transverse momentum spectra of charged particles in pPb collisions at $\sqrt{s_{\mathrm{NN}}} = 5.02$ TeV

CMS Collaboration*

CERN, Geneva, Switzerland

Received: 18 February 2015 / Accepted: 1 May 2015

Abstract Transverse momentum spectra of charged particles are measured by the CMS experiment at the CERN LHC in pPb collisions at $\sqrt{s_{\mathrm{NN}}} = 5.02$ TeV, in the range $0.4 < p_{\mathrm{T}} < 120$ GeV/c and pseudorapidity $|\eta_{\mathrm{CM}}| < 1.8$ in the proton–nucleon center-of-mass frame. For $p_{\mathrm{T}} < 10$ GeV/c, the charged-particle production is asymmetric about $\eta_{\mathrm{CM}} = 0$, with smaller yield observed in the direction of the proton beam, qualitatively consistent with expectations from shadowing in nuclear parton distribution functions (nPDF). A pp reference spectrum at $\sqrt{s} = 5.02$ TeV is obtained by interpolation from previous measurements at higher and lower center-of-mass energies. The p_{T} distribution measured in pPb collisions shows an enhancement of charged particles with $p_{\mathrm{T}} > 20$ GeV/c compared to expectations from the pp reference. The enhancement is larger than predicted by perturbative quantum chromodynamics calculations that include antishadowing modifications of nPDFs.

1 Introduction

The central goal of the heavy ion experimental program at ultra-relativistic energies is to create a system of deconfined quarks and gluons, known as a quark–gluon plasma (QGP), and to study its properties as it cools down and transitions into a hadron gas. A key tool in the studies of the QGP is the phenomenon of jet quenching [1], in which the partons produced in hard scatterings lose energy through gluon radiation and elastic scattering in the hot and dense partonic medium [2]. Since high transverse momentum quarks and gluons fragment into jets of hadrons, one of the observable consequences of parton energy loss is the suppression of the yield of high-p_{T} particles in comparison to their production in proton–proton (pp) collisions. This suppression, studied as a function of the p_{T} and pseudorapidity (η) of the produced particle, is usually quantified in terms of the nuclear modification factor, defined as

$$R_{\mathrm{AB}}(p_{\mathrm{T}}, \eta) = \frac{1}{\langle \mathrm{T_{AB}} \rangle} \frac{\mathrm{d}^2 N^{\mathrm{AB}}/\mathrm{d}p_{\mathrm{T}}\,\mathrm{d}\eta}{\mathrm{d}^2 \sigma^{\mathrm{pp}}/\mathrm{d}p_{\mathrm{T}}\,\mathrm{d}\eta}, \quad (1)$$

where N^{AB} is the particle yield in a collision between nuclear species A and B, σ^{pp} is the corresponding cross section in pp collisions, and $\langle \mathrm{T_{AB}} \rangle$ is the average nuclear overlap function [3] in the AB collision (in the case of proton–nucleus collisions, the quantity $\langle \mathrm{T_{AB}} \rangle = \langle \mathrm{T_{pA}} \rangle$ is called average nuclear thickness function). If nuclear collisions behave as incoherent superpositions of nucleon–nucleon collisions, a ratio of unity is expected. Departures from unity are indicative of final-state effects such as parton energy loss, and/or initial-state effects such as modifications of the nuclear parton distribution functions (nPDF) [4]. The nPDFs are constrained by measurements in lepton–nucleus deep-inelastic scattering (DIS) and Drell–Yan (DY) production of dilepton pairs from $\mathrm{q\bar{q}}$ annihilation in proton–nucleus collisions [5]. In the small parton fractional momentum regime ($x \lesssim 0.01$), the nPDFs are found to be suppressed relative to the proton PDFs, a phenomenon commonly referred to as "shadowing" [6]. At small x, where the parton distributions are described theoretically by non-linear evolution equations in x, gluon saturation is predicted by the color glass condensate models [7–9]. For the x regime $0.02 \lesssim x \lesssim 0.2$, the nPDFs are enhanced ("antishadowing") relative to the free-nucleon PDFs [5].

To gain access to the properties of the QGP produced in heavy ion collisions it is necessary to separate the effects directly related to the hot partonic medium from those that are not, referred to as "cold nuclear matter" effects. In particular, nPDF effects are expected to play an important role in the interpretation of nuclear modification factors at the CERN LHC. Unfortunately, the existing nuclear DIS and DY measurements constrain only poorly the gluon distributions over much of the kinematic range of interest. High-p_{T} hadron production in proton–nucleus (or deuteron–nucleus) collisions provides a valuable reference for nucleus–nucleus collisions, as it probes initial-state nPDF modifications over a wide kinematic range and is expected to be largely free from the final-state effects that accompany QGP production [10].

* e-mail: cms-publication-committee-chair@cern.ch

Published online: 29 May 2015

The measurements of the nuclear modification factors of neutral pions and charged hadrons in the most central gold–gold (AuAu) collisions at the relativistic heavy ion collider (RHIC) [11–14] revealed a large suppression at high p_{T}, reaching an R_{AA} as low as 0.2. In contrast, no such suppression was found at mid-rapidity in deuteron–gold collisions at the same energy [15–18]. These findings established parton energy loss, rather than initial-state effects [19], as the mechanism responsible for the modifications observed in AuAu collisions.

At the LHC, the charged-particle suppression in lead–lead (PbPb) collisions persists at least up to a p_{T} of 100 GeV/c [20,21]. In proton–lead (pPb) collisions, the ALICE Collaboration reported no significant deviations from unity in the charged-particle R_{pPb} up to $p_{\mathrm{T}} \approx 50$ GeV/c [22]. The analysis presented here used data from CMS to extend the measurement of the charged-particle R_{pPb} out to $p_{\mathrm{T}} \approx 120$ GeV/c, with the aim of evaluating initial-state effects over a kinematic range similar to that explored through measurements in PbPb collisions [20].

Proton–nucleus collisions have already been used to assess the impact of cold nuclear matter on jet production at the LHC. The transverse momentum balance, azimuthal angle correlations, and pseudorapidity distributions of dijets have been measured as a function of the event activity, and no significant indication of jet quenching was found [23]. When normalized to unity, the minimum-bias dijet pseudorapidity distributions are found to be consistent with next-to-leading-order (NLO) perturbative quantum chromodynamic (pQCD) calculations only if nPDF modifications are included [24]. Similarly, inclusive jet R_{pPb} measurements are also found to be consistent with NLO pQCD predictions that include nPDF modifications [25,26]. The measurement of the charged-particle spectra presented in this paper provides a comparison to theory that is sensitive to smaller x values than those accessible in the jet measurements. However, it should be noted that the charged-particle R_{pPb} is dependent upon non-perturbative hadronization effects, some of which, such as gluon fragmentation into charged hadrons, are poorly constrained at the LHC energies [27].

The p_{T} distributions of inclusive charged particles in pPb collisions at a nucleon–nucleon center-of-mass energy of 5.02 TeV are presented in the range of $0.4 < p_{\mathrm{T}} < 120$ GeV/c. The measurement is performed in several pseudorapidity intervals over $|\eta_{\mathrm{CM}}| < 1.8$. Here η_{CM} is the pseudorapidity in the proton–nucleon center-of-mass frame. The nuclear modification factor is studied at mid-rapidity, $|\eta_{\mathrm{CM}}| < 1$, and the forward-backward asymmetry of the yields, Y_{asym}, defined as

$$Y_{\mathrm{asym}}^{(a,b)}(p_{\mathrm{T}}) = \frac{\int_{-b}^{-a} \mathrm{d}\eta_{\mathrm{CM}}\, \mathrm{d}^2 N_{\mathrm{ch}}(p_{\mathrm{T}})/\mathrm{d}\eta_{\mathrm{CM}}\, \mathrm{d}p_{\mathrm{T}}}{\int_{a}^{b} \mathrm{d}\eta_{\mathrm{CM}}\, \mathrm{d}^2 N_{\mathrm{ch}}(p_{\mathrm{T}})/\mathrm{d}\eta_{\mathrm{CM}}\, \mathrm{d}p_{\mathrm{T}}}, \tag{2}$$

is presented for three pseudorapidity intervals, where a and b are positive numbers, and N_{ch} is the yield of charged particles.

Due to their wide kinematic coverage, the measurements are expected to provide information about the nPDFs in both the shadowing and antishadowing regions. In particular, the effects of shadowing are expected to be more prominent at forward pseudorapidities (in the proton-going direction), where smaller x fractions in the nucleus are accessed.

In the absence of other competing effects, shadowing in the Pb nPDFs would result in values of $Y_{\mathrm{asym}} > 1$ at low p_{T} (i.e., small x). The effects of antishadowing can be probed with the R_{pPb} measurement at larger p_{T} values of $30 \lesssim p_{\mathrm{T}} \lesssim 100$ GeV/c that correspond approximately to $0.02 \lesssim x \lesssim 0.2$. Antishadowing in the nPDFs may increase the yield of charged particles in pPb collisions compared with expectations from the yield in pp collisions.

2 Data selection and analysis

2.1 Experimental setup

A detailed description of the CMS detector can be found in Ref. [28]. The CMS experiment uses a right-handed coordinate system, with the origin at the nominal interaction point (IP) at the center of the detector, and the z axis along the beam direction. The silicon tracker, located within the 3.8 T magnetic field of the superconducting solenoid, is used to reconstruct charged-particle tracks. Consisting of 1440 silicon pixel detector modules and 15,148 silicon strip detector modules, totaling about 10 million silicon strips and 60 million pixels, the silicon tracker measures the tracks of charged particles within the pseudorapidity range $|\eta| < 2.5$. It provides an impact parameter resolution of $\approx 15\,\mu$m and a p_{T} resolution of about 1.5 % for particles with p_{T} of 100 GeV/c. An electromagnetic calorimeter (ECAL) and a hadron calorimeter (HCAL) are also located inside the solenoid. The ECAL consists of more than 75,000 lead tungstate crystals, arranged in a quasi-projective geometry; the crystals are distributed in a barrel region ($|\eta| < 1.48$) and in two endcaps that extend out to $|\eta| \approx 3.0$. The HCAL barrel and endcaps, hadron sampling calorimeters composed of brass and scintillator plates, have an acceptance of $|\eta| \lesssim 3.0$. The hadron forward calorimeters (HF), consisting of iron with quartz fibers read out by photomultipliers, extend the calorimeter coverage out to $|\eta| = 5.2$, and are used in offline event selection. Beam Pick-up Timing for the eXperiments (BPTX) devices were used to trigger the detector readout. They are located around the beam pipe at a distance of 175 m from the IP on either side, and are designed to provide precise information on the LHC bunch structure and timing of the incoming beams. The

detailed Monte Carlo (MC) simulation of the CMS detector response is based on GEANT4 [29].

This measurement is based on a data sample corresponding to an integrated luminosity of 35 nb^{-1}, collected by the CMS experiment in pPb collisions during the 2013 LHC running period. The center-of-mass energy per nucleon pair was $\sqrt{s_{\text{NN}}} = 5.02$ TeV, corresponding to per-nucleon beam energies of 4 TeV and 1.58 TeV for protons and lead nuclei, respectively. The data were taken with two beam configurations. Initially, the Pb nuclei traveled in the counterclockwise direction, while in the second data-taking period, the beam directions were reversed. Both data sets, the second one being larger by approximately 50 %, were analyzed independently, yielding compatible results. To combine data from the two beam configurations, results from the first data-taking period are reflected along the z-axis, so that in the combined analysis, the proton travels in the positive z and η directions. In this convention, massless particles emitted at $\eta_{\text{CM}} = 0$ in the nucleon–nucleon center-of-mass frame will be detected at $\eta_{\text{lab}} = 0.465$ in the laboratory frame. A symmetric region about $\eta_{\text{CM}} = 0$ is used in the data analysis, resulting in a selected pseudorapidity range of $|\eta_{\text{CM}}| < 1.8$.

2.2 Event selection

The CMS online event selection employs a hardware-based level-1 (L1) trigger and a software-based high-level trigger (HLT). A minimum-bias sample is selected first by the L1 requirement of a pPb bunch crossing at the IP (as measured by the BPTX), and an HLT requirement of at least one reconstructed track with $p_{\text{T}} > 0.4$ GeV/c in the pixel tracker. For most of the 5.02 TeV data collection, the minimum-bias trigger is significantly prescaled because of the high instantaneous LHC luminosity. To increase the p_{T} reach of the measurement, a set of more selective triggers is also used: additional L1 requirements are imposed to select events that have at least one reconstructed calorimeter jet with an uncorrected transverse energy of $E_{\text{T}} > 12$ GeV, and $E_{\text{T}} > 16$ GeV. These event selections are complemented by additional HLT requirements that select events based on the presence of at least one track with $p_{\text{T}} > 12$ GeV/c (for L1 $E_{\text{T}} > 12$ GeV), or with $p_{\text{T}} > 20$ or 30 GeV/c (for L1 $E_{\text{T}} > 16$ GeV) reconstructed in the pixel and strip tracker.

The above triggering strategy allows for the optimization of the data-taking rate while adequately sampling all p_{T} regions, including collecting all events containing very high-p_{T} tracks. The track trigger with a p_{T} threshold of 12 GeV/c records about 140 times more events with high-p_{T} tracks than the minimum-bias trigger, the track $p_{\text{T}} > 20$ GeV/c trigger enhances this with an additional factor of about 8, while the track $p_{\text{T}} > 30$ GeV/c trigger that is not prescaled, increases the number of events with a high-p_{T} track by yet another factor of about 2.

In the offline analysis, additional requirements are applied. Events are accepted if they have (i) at least one HF calorimeter tower on both the positive and negative sides of the HF with more than 3 GeV of total energy, (ii) at least one reconstructed collision vertex with two or more associated tracks, and (iii) a maximum distance of 15 cm along the beam axis between the vertex with the largest number of associated tracks and the nominal IP. Beam-related background is suppressed by rejecting events where less than 25 % of all reconstructed tracks are of good quality [30].

An event-by-event weight factor accounts for correcting the measured charged-particle spectra in pPb collisions to a detector-independent class of collisions termed as "double-sided" (DS) events, which are very similar to those that pass the offline selection described above. A DS event is defined as a collision producing at least one particle in the pseudorapidity range $-5 < \eta_{\text{lab}} < -3$ and another in the range $3 < \eta_{\text{lab}} < 5$, each with proper lifetime $\tau > 10^{-18}$ s and energy $E > 3$ GeV [31]. The performance of the minimum-bias and high-p_{T} single-track triggers, as well as the offline criteria in selecting DS events, is evaluated with simulations using the HIJING MC generator [32], version 1.383 [33], and the correction factors are computed as a function of the event multiplicity. An efficiency of 99 % is obtained for the minimum-bias trigger and a negligible correction (i.e., 100 % efficiency) for the high-p_{T} track-triggered events. The correction factor is also evaluated using an EPOS [34] simulation and, based on the difference between both generators, a slightly p_{T}-dependent systematic uncertainty of 1 % is assigned to the final spectra.

During the pPb data taking period, about 3 % of the recorded events contained more than one pPb collision. To reduce potential bias in the measurements arising from such "pileup", events with multiple reconstructed vertices are removed if the longitudinal distance between the vertices along the beamline is greater than a specific value that is related to the uncertainty of the vertex position. This value is also dependent on the number of tracks associated with each vertex and ranges from 0.2 cm for vertex pairs with at least 25 tracks associated with each vertex, to 3 cm for vertex pairs with only 3 tracks associated with the vertex having the fewest associated tracks. Simulated HIJING events are used to tune the pileup-rejection algorithm in order to reduce the number of erroneously eliminated single-collision events to a negligible fraction, and still maintain a high rejection efficiency for genuine pileup events. The pileup-rejection efficiency is found to be 92 ± 2 %, which is confirmed by using a low bunch intensity control sample in data.

To obtain inclusive particle spectra up to $p_{\text{T}} \approx 120$ GeV/c, data recorded with the minimum-bias and high-p_{T} track triggers must be combined appropriately. The corresponding weight factors are computed by counting the number of events that contain leading tracks (defined as the track with

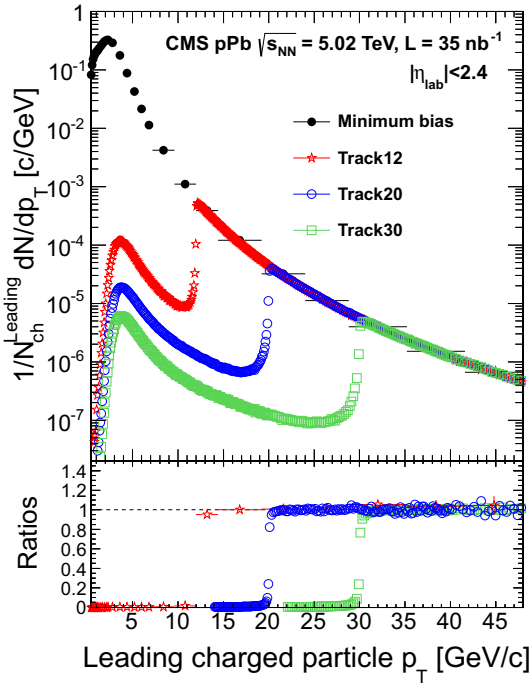

Fig. 1 *Top* Charged-particle yields for the different triggers normalized to the number of leading charged particles with $p_T > 0.4$ GeV/c in double-sided events, $N_{ch}^{Leading}$, as a function of leading-track p_T. The track-triggered distributions are normalized by the number of leading tracks in regions not affected by the rapid rise of the trigger efficiency near threshold. *Bottom* Ratios of the leading-track p_T distributions for the four different triggers. The *stars* indicate the ratio of the 12 GeV/c over the minimum-bias samples, the *circles* the 20 over the 12 GeV/c samples, and the *squares* the ratio of the 30 over the 20 GeV/c track-triggered spectra

the highest p_T in the event) in the range of $|\eta_{lab}| < 2.4$ with p_T values in regions not affected by trigger thresholds, i.e., where the trigger efficiency of the higher-threshold trigger is constant relative to that of the lower-threshold trigger. The ratio of the number of such events in the two triggered sets of data are used as weight factors. For example, the region above which the track trigger with a p_T threshold of 12 GeV/c has constant efficiency is determined by comparing the p_T distribution of the leading tracks to that of the minimum-bias data. Similarly, the constant efficiency region of the 20 GeV/c track trigger is determined by comparison to the 12 GeV/c track trigger, and the 30 GeV/c trigger to the 20 GeV/c trigger. The regions of constant efficiency for each trigger, as a function of leading charged-particle p_T, are shown in Fig. 1. The 12, 20, and 30 GeV/c triggers have constant efficiencies above a leading charged-particle p_T of 14, 22, and 32 GeV/c, respectively. The weight factors are then computed using the leading-track p_T classes of $14 < p_T < 22$ GeV/c, $22 < p_T < 32$ GeV/c, and $p_T > 32$ GeV/c for the three high-p_T triggers. The combined uncertainty in these normalizations is dominated by the matching of the 12 GeV/c track-triggered events to the minimum-bias events.

Some events selected by the track triggers in Fig. 1 are observed to result in a leading charged-particle p_T below the corresponding trigger threshold. This can happen if the η of the track above threshold is outside the η range considered in the analysis, and because the final track reconstruction—described in Sect. 2.3—is more robust and selective than the fast-tracking algorithm implemented in the HLT. When the HLT selects an event based on a misreconstructed track, it is often the case that the track is not found in the final reconstruction. To determine the inclusive particle spectrum, events are first uniquely classified into leading-track p_T classes in the pseudorapidity range in which the spectrum is being measured. The spectra are constructed by taking events from the minimum-bias, 12 GeV/c track, 20 GeV/c track, and 30 GeV/c track trigger, respectively, for each bin. A 4 % systematic uncertainty on the possible trigger-bias effect is estimated from MC simulations. This procedure was verified in a data-driven way by constructing a charged-particle spectrum from an alternative combination of event samples triggered by reconstructed jets. Both final spectra, triggered by tracks and jets, are found to be consistent within the associated systematic uncertainty.

2.3 Track reconstruction

The p_T distribution in this analysis corresponds to that of primary charged particles, defined as all charged particles with a mean proper lifetime greater than 1 cm/c, including the products of strong and electromagnetic decays, but excluding particles originating from secondary interactions in the detector material. Weak-decay products are considered primary charged particles only if they are the daughters of a particle with a mean proper lifetime of less than 1 cm/c, produced in the collision.

Charged particles are reconstructed using the standard CMS combinatorial track finder [35]. The proportion of misreconstructed tracks in the sample is reduced by applying an optimized set of standard tracking-quality selections, as described in Ref. [35]. A reconstructed track is considered as a primary charged-particle candidate if the statistical significance of the observed distance of closest approach between the track and the reconstructed collision vertex is less than three standard deviations, under the hypothesis that the track originated from this vertex. In case an event has multiple reconstructed collision vertices but is not rejected by the pileup veto, the track distance is evaluated relative to the best reconstructed collision vertex, defined as the one associated with the largest number of tracks, or the one with the lowest χ^2 if multiple vertices have the same number of associated tracks. To remove tracks with poor momentum reconstruction, the relative uncertainty of the momentum measurement $\sigma(p_T)/p_T$ is required to be less than 10 %. Only tracks that fall in the kinematic range of $|\eta_{lab}| < 2.4$ and $p_T > 0.4$ GeV/c

are selected for analysis to ensure high tracking efficiency (70–90 %) and low misreconstruction rates (<2 %).

The yields of charged particles in each p_{T} and η bin are weighted by a factor that accounts for the geometrical acceptance of the detector, the efficiency of the reconstruction algorithm, the fraction of tracks corresponding to a non-primary charged particle, the fraction of misreconstructed tracks that do not correspond to any charged particle, and the fraction of multiply-reconstructed tracks, which belong to the same charged particle.

The various correction terms are estimated using simulated minimum-bias pPb events from the HIJING event generator. To reduce the statistical uncertainty in the correction factors at high p_{T}, samples of HIJING events are also mixed with pp dijet events from the PYTHIA MC generator [36] (version 6.423, tune D6T with CTEQ6L1 PDF for 2.76 TeV, tune Z2 for 7 TeV [37]).

The efficiency of the charged-particle reconstruction as well as the misreconstruction rates are also evaluated using pPb events simulated with EPOS. Differences between the two MC models are mostly dominated by the fraction of charged particles consisting of strange and multi-strange baryons that are too short-lived to be reconstructed unless they are produced at very high p_{T}. Such differences in particle species composition, which are largest for particles with $3 \lesssim p_{\mathrm{T}} \lesssim 14$ GeV/c, are propagated as a systematic uncertainty in the measured spectra. Below this p_{T} range, the strange baryons are only a small fraction of the inclusive charged particles in either model, and the difference in reconstruction efficiency between particle species has less impact at even larger p_{T}, as high-p_{T} multi-strange baryons can be directly tracked with high efficiency. Additional checks were performed by changing cutoffs imposed during track selection and in the determination of the corresponding MC-based corrections. The corresponding variations in the corrected yields amount to 1.2–4.0 % depending on the p_{T} region under consideration, and are included in the systematic uncertainty.

Finite bin-widths and finite transverse momentum resolution can deform a steeply falling p_{T} spectrum. The data are corrected for the finite bin-width effect as they will be compared to a pp reference spectrum obtained by interpolation. The binning corrections are derived by fitting the measured distribution and using the resulting fit function as a probability distribution to generate entries in a histogram with the same p_{T} binning as used in the measurement. The correction factors are then obtained from the ratio of entries in the bins of the histogram to the fit function evaluated at the centers of the bins. This correction amounts to 0–12 %, depending on p_{T}. A similar method is used to evaluate the "smearing" effect of the finite p_{T} resolution on the binned distributions. It is found that the momentum measurement, which has a resolution of $\sigma(p_{\mathrm{T}})/p_{\mathrm{T}} \approx 1.5$ % near a p_{T} of 100 GeV/c, is sufficiently precise to only have a negligible effect on the measured spectra and therefore no correction factor is applied. To account for possible incorrect determination of the momentum resolution from the simulation, the effects were again evaluated after increasing the value of $\sigma(p_{\mathrm{T}})/p_{\mathrm{T}}$ by an additional 0.01, which produces a maximal distortion in the spectrum at a given p_{T} of less than 1 %.

2.4 Proton–proton reference spectrum

The pPb collisions occur at a center-of-mass energy of 5.02 TeV per nucleon pair. At this collision energy, no proton–proton collisions have been provided by particle accelerators yet. The pp results closest in center-of-mass energy ($\sqrt{s}$) and with similar acceptance are those measured at 2.76 and 7 TeV by the CMS experiment [20,38]. The determination of the nuclear modification factor R_{AB} resides in an interpolated reference spectrum to be constructed from data at higher and lower energies. We follow the direct interpolation method developed in Ref. [38] using measured p_{T} spectra from inelastic collisions with $|\eta| < 1.0$ at $\sqrt{s} = 0.63$, 1.8, and 1.96 TeV collision energies from CDF [39,40], and 0.9, 2.76, and 7 TeV collision energies from CMS [20,38]. This interpolation can be performed either as a function of p_{T} or as a function of $x_{\mathrm{T}} \equiv 2p_{\mathrm{T}}c/\sqrt{s}$.

Since the p_{T} or x_{T} values of the input data points are often different for each measurement performed at the various collision energies, each spectrum must first be fitted as a function of p_{T} or x_{T}. An interpolation is performed by fitting each of the spectra to a power-law dependence, and the resulting residuals to first- or third-order splines. The fitted spectra are then interpolated to determine the value of the reference spectrum at $\sqrt{s} = 5.02$ TeV using a second-order polynomial in the plane of the log-log invariant production *vs.* $\sqrt{s}$, as shown in Fig. 2. For the p_{T}-based direct interpolation, data from only two of the six spectra are available at $p_{\mathrm{T}} > 30$ GeV/c, which implies that the p_{T}-based direct interpolation is well constrained only at low p_{T}. On the other hand, the x_{T}-based interpolation is well constrained at high p_{T} for $\sqrt{s} = 5.02$ TeV, so it is natural to combine the reference distributions from these two direct interpolation methods.

The final pp reference spectrum is obtained by combining the p_{T}- and x_{T}-based reference spectra as follows. The p_{T}-based reference is chosen for p_{T} below 12.5 GeV/c, and the x_{T}-based result above 13.5 GeV/c; between these two p_{T} values a linear weighting is implemented for the two references. The systematic uncertainty in the pp reference spectrum is determined through changing both the specific method of interpolation, as well as the underlying pp reference data within their statistical and systematic uncertainties. The systematic uncertainty is dominated by the interpolation method, and is determined by comparing the combined p_{T}- and x_{T}-based reference spectra to the reference spectra obtained solely from the p_{T} or x_{T} distributions, and also from a refer-

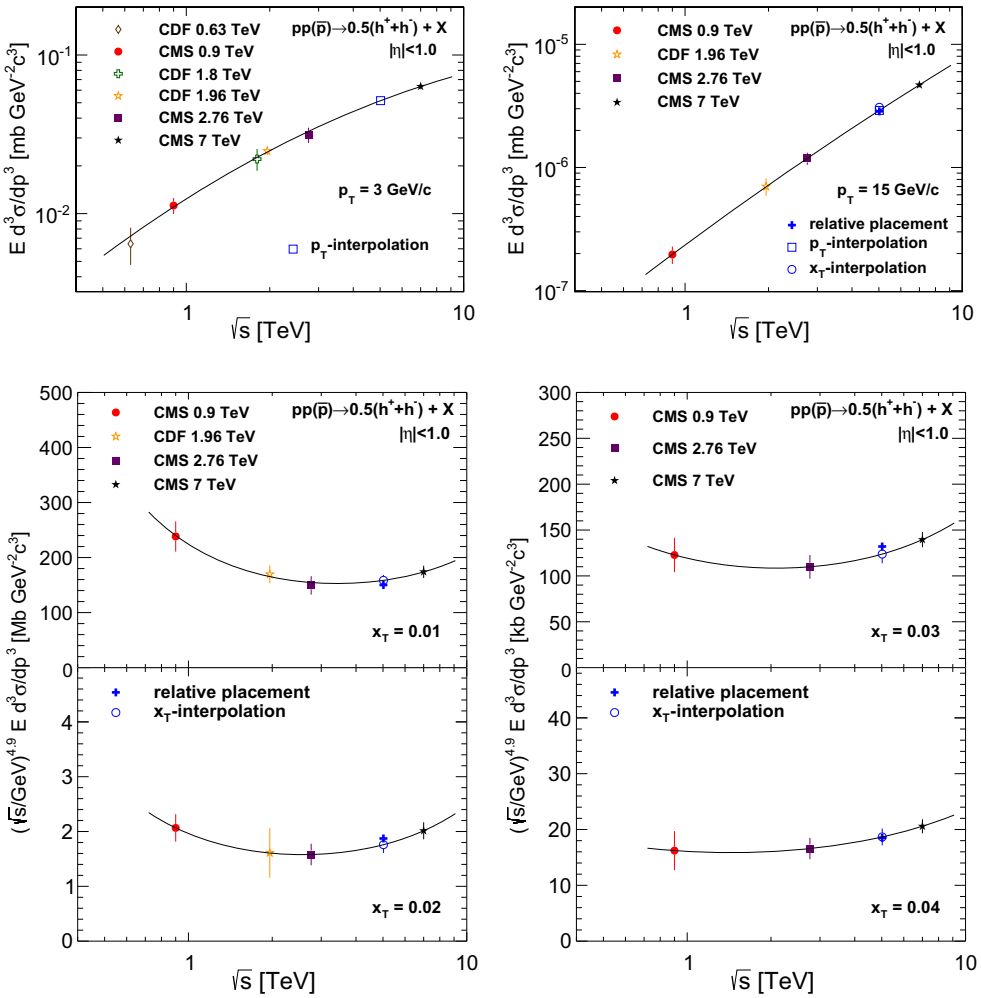

Fig. 2 Examples of interpolations between measured charged-particle differential cross sections at different $\sqrt{s}$ for p_{T} values of 3 and 15 GeV/c (*top left* and *right*), x_{T} values of 0.01 and 0.02 (*bottom left*), and x_{T} values of 0.03 and 0.04 (*bottom right*). These x_{T} values correspond to $p_{\mathrm{T}} \approx 25$, 50, 75, and 100 GeV/$c$ at $\sqrt{s} = 5.02$ TeV. The second-order polynomial fits, performed in the plane of the log–log invariant production vs. $\sqrt{s}$, are shown by the *solid lines*. The *open squares* and *circles*, and the *filled crosses* represent interpolated cross section values at 5.02 TeV using different methods: p_{T}-based interpolation, x_{T}-based interpolation, and relative placement, respectively. The *error bars* on the interpolated points represent the uncertainties in the fit

ence spectrum determined by a "relative placement" method. In the latter, the reference spectrum is obtained by computing where the 5.02 TeV spectrum is situated with respect to the 2.76 and 7 TeV spectra in PYTHIA, and applying the computed placement factors to the measured 2.76 and 7 TeV spectra. The placement factors are determined by taking the value of the 5.02 TeV PYTHIA spectrum, subtracting the value of the 2.76 TeV spectrum, and dividing by the difference between the 7 and the 2.76 TeV spectra. This process is then reversed by using the computed placement factors from PYTHIA, and replacing the 2.76 and 7 TeV PYTHIA spectra with the measured ones to determine the interpolated 5.02 TeV spectrum. Additionally, the NLO-based center-of-mass energy rescaling proposed in Ref. [41] is found to yield results consistent within the uncertainties of the other employed methods. The uncertainty in the pp reference distribution due to the interpolation method is estimated to amount to 10 %, which captures the overall point-to-point variations in all of the interpolation and scaling methods employed. The contribution from the uncertainties in the underlying pp input data corresponds to 6 %. These numbers are added in quadrature, resulting in the 12 % uncertainty quoted for the $\sqrt{s} = 5.02$ TeV interpolated pp reference spectrum.

3 Systematic uncertainties

A summary of all the contributions to systematic uncertainties in the p_{T} spectra, R^{*}_{pPb}, and Y_{asym} are given in Table 1. The asterisk symbol is introduced to denote that an interpolated, rather than measured, pp reference spectrum is used to construct the nuclear modification factor. Aside

Table 1 Systematic uncertainties in the measurement of charged-particle spectra, R^*_{pPb}, and Y_{asym}

Source	Uncertainty (%)
Trigger efficiency	1.0
Momentum resolution	1.0
Particle species composition	1–10.0 (0.5–5)
Track misreconstruction rate	1.0
Track selection	1.2–4.0
Spectra relative normalization	0.0–1.0
Trigger bias	0.0–4.0
Total (spectra)	2.2–10.9
pp interpolation	12.0
Total (R^*_{pPb})	12.2–16.2
$\langle \mathrm{T_{pPb}} \rangle$ average nuclear thickness	4.8
Total (Y_{asym} $0.3 < \lvert\eta_{\mathrm{CM}}\rvert < 0.8$)	2.0–3.0
Total (Y_{asym} $0.8 < \lvert\eta_{\mathrm{CM}}\rvert < 1.3$)	2.0–5.0
Total (Y_{asym} $1.3 < \lvert\eta_{\mathrm{CM}}\rvert < 1.8$)	2.0–5.0

The ranges quoted refer to the variations of the uncertainties as a function of p_{T}. Values in parentheses denote the negative part of the asymmetric uncertainty where applicable. The total uncertainties of the measured pPb and the interpolated pp spectra, as a function of p_{T}, are shown in the lower panel of Fig. 3

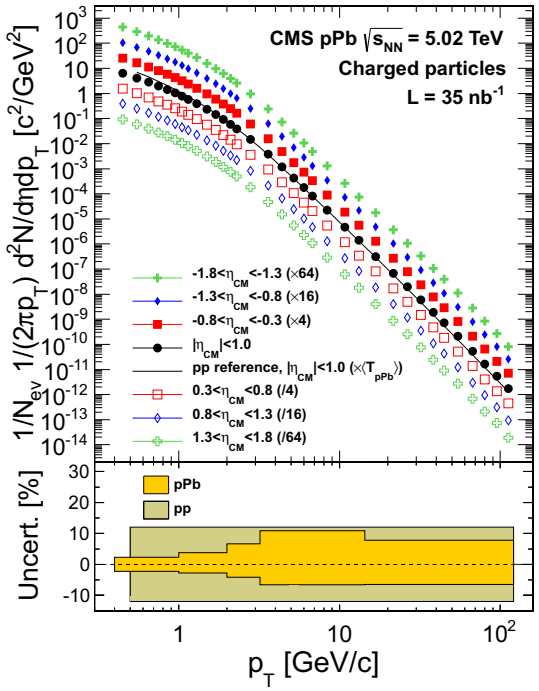

Fig. 3 *Top* Measured charged-particle transverse momentum spectra in pPb collisions at $\sqrt{s_{\mathrm{NN}}} = 5.02$ TeV for: $|\eta_{\mathrm{CM}}| < 1.0$, $0.3 < \pm\eta_{\mathrm{CM}} < 0.8$, $0.8 < \pm\eta_{\mathrm{CM}} < 1.3$, and $1.3 < \pm\eta_{\mathrm{CM}} < 1.8$, and the interpolated pp reference spectrum in $|\eta_{\mathrm{CM}}| < 1$, normalized to the number of double-sided events. Positive pseudorapidity values correspond to the proton beam direction. The spectra have been scaled by the quoted factors to provide better visibility. *Bottom* Systematic uncertainties in the measured pPb and interpolated pp spectra, as a function of p_{T} (see text)

from the uncertainty from the spectra relative normalization and average nuclear thickness, all uncertainties are determined by taking the approximate maximum deviation from the central value found for the given source. For the particle species uncertainty, an asymmetric uncertainty band is quoted because the maximum deviation above the central value of the measurement is much larger than the maximum deviation below. For the purpose of determining the significance of observed features in the measurement, the uncertainties are conservatively treated as following a Gaussian distribution with a root mean square given by the value of the uncertainty as determined above.

The degree of correlation among different uncertainties is described next. For the spectra and R^*_{pPb} measurements, the uncertainty in the efficiency of the single-track trigger and offline requirements in selecting DS events is largely a normalization uncertainty, although it also slightly affects the shape of the spectrum for $p_{\mathrm{T}} \lesssim 3$ GeV/c. The uncertainty from the contribution of the various particle species to the unidentified spectrum has the most significant effect in the region $3 < p_{\mathrm{T}} < 14$ GeV/c and can impact the shape of the spectrum in a smooth fashion. At high p_{T}, this effect is less prominent because, due to time dilation, unstable particles have a higher probability of traversing the inner tracker before decaying and therefore a higher probability of being reconstructed. Therefore, from this uncertainty the lower bound on the pPb spectra measurement at higher p_{T} is 2.5 % below the central value, which corresponds to no unstable particles being produced. Uncertainty in track misreconstruction can also affect the shape of the measured spectrum, as the misreconstructed fraction of high-p_{T} particles is sensitive to large occupancy in the silicon tracker within the cones of high-energy jets. The uncertainty in tracking selection can also affect the shape of the spectrum by raising or lowering the measured values at high p_{T}, without changing the low-p_{T} values, as high-p_{T} tracks are more sensitive to possible mismodeling of detector alignment than low-p_{T} tracks. The uncertainty in the relative normalization of spectra is computed from the normalization factors involved in the combination of the p_{T} distributions from different triggers. This uncertainty only applies for selected p_{T} regions, and may raise or lower the spectrum above $p_{\mathrm{T}} = 14$ GeV/c by a constant factor of 1 % relative to the lower-p_{T} part of the spectrum. The uncertainty from potential biases of the method used to combine triggers can also affect the shape of the spectrum above $p_{\mathrm{T}} = 14$ GeV/c.

For the R^*_{pPb} measurement, the uncertainty in the average nuclear thickness function [3] can influence the R^*_{pPb} curve by a constant multiplicative factor. The uncertainty from the pp interpolation is strongly correlated among points

close together in p_T, while some partial correlation remains throughout the whole p_T region, even for very different p_T values.

For the forward-backward asymmetry measurements, most of these uncertainties cancel in part or in full when the ratio of the spectra is taken. The remaining uncertainty in the detector acceptance and tracking efficiency can change the shape of the forward-backward asymmetry, particularly at high p_T.

4 Results

The measured charged-particle yields in double-sided pPb collisions at $\sqrt{s_{NN}} = 5.02$ TeV are plotted in Fig. 3 for the $|\eta_{CM}| < 1.0$, $0.3 < \pm\eta_{CM} < 0.8$, $0.8 < \pm\eta_{CM} < 1.3$, and $1.3 < \pm\eta_{CM} < 1.8$ pseudorapidity ranges. Positive (negative) pseudorapidity values correspond to the proton (lead) beam direction. To improve the visibility of the results, the spectra at different pseudorapidities have been scaled up and down by multiple factors of 4 relative to the data for $|\eta_{CM}| < 1$. The relative uncertainties for the pPb and the pp spectra are given in the bottom panel.

The measurement of the charged-particle nuclear modification factor of Eq. (1) requires a rescaling of the pp cross section by the average nuclear thickness function in minimum-bias pPb collisions. This factor amounts to $\langle T_{pPb} \rangle = (0.0983 \pm 0.0044)\,\text{mb}^{-1}$ for inelastic pPb collisions and is obtained from a Glauber MC simulation [3,42], where the Pb nucleus is described using a Woods-Saxon distribution with nuclear radius 6.62 ± 0.13 fm and skin depth of 0.546 ± 0.055 fm [3,43]. As double-sided events correspond to 94–97 % of inelastic collisions based on HIJING and EPOS MC computations [31], the value of $\langle T_{pPb} \rangle$ would be about 5 % higher for double-sided events.

The charged-particle R^*_{pPb} at mid-rapidity ($|\eta_{CM}| < 1$) is plotted in Fig. 4 as a function of p_T. The shaded band at unity and $p_T \approx 0.6$ represents the uncertainty in the Glauber calculation of $\langle T_{pPb} \rangle$. The smaller uncertainty band around the measured values shows the fully correlated uncertainties from the following sources: spectra relative normalization, track selection, and trigger efficiency. The total systematic uncertainties are shown by the larger band around the measured values (Table 1). The nuclear modification factor shows a steady rise to unity at $p_T \approx 2$ GeV/c, then remains constant at unity up to approximately 20 GeV/c, and rises again at higher p_T, reaching a maximum value around 1.3–1.4 above 40 GeV/c.

The fact that the nuclear modification factor is below unity for $p_T \lesssim 2$ GeV/c is anticipated since particle production in this region is dominated by softer scattering processes, that are not expected to scale with the nuclear thickness function. In the intermediate p_T range (2–5 GeV/c), no

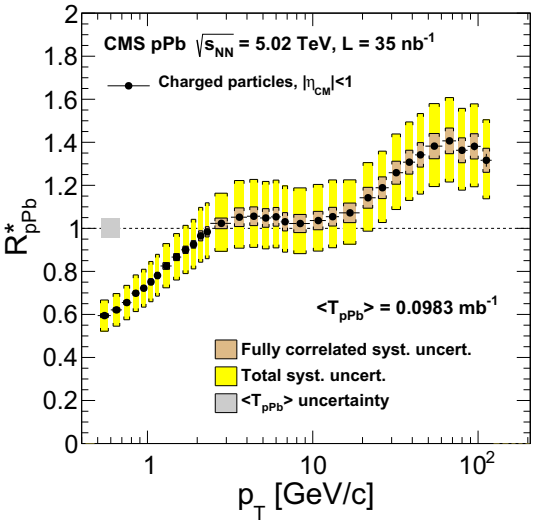

Fig. 4 Measured nuclear modification factor as a function of p_T for charged particles produced in $|\eta_{CM}| < 1$. The *shaded band* at unity and $p_T \approx 0.6$ represents the uncertainty in the Glauber calculation of $\langle T_{pPb} \rangle$. The *smaller uncertainty band* around the data points shows the uncertainty from effects (combining spectra, track selection, and trigger efficiency) that are fully correlated in specific p_T regions. The total systematic uncertainties, dominated by uncertainty in the pp interpolation, are shown by the *larger band* (see Table 1)

significant deviation from unity is found in the R^*_{pPb} ratio. There are several prior measurements that suggest an interplay of multiple effects in this p_T region. At lower collision energies, an enhancement ("Cronin effect" [44]) has been observed [15–18] that is larger for baryons than for mesons, and is stronger in the more central collisions. This enhancement has been attributed to a combination of initial-state multiple scattering effects, causing momentum broadening, and hadronization through parton recombination (a final-state effect) [45] invoked to accommodate baryon/meson differences. Recent results from pPb collisions at $\sqrt{s_{NN}} = 5.02$ TeV [31,46–49] and from dAu collisions at $\sqrt{s_{NN}} = 200$ GeV [50,51] suggest that collective effects may also play a role in the intermediate-p_T region. Most theoretical models do not predict a Cronin enhancement in this p_T range at LHC energies as the effect of initial-state multiple scattering is compensated by nPDF shadowing [52].

In Fig. 5, the CMS measurement is compared to the result of an NLO pQCD calculation [53] for charged particles produced at mid-rapidity. The calculation uses the CTEQ10 [54] free-proton PDF, the EPS09 nPDF [4], and the fDSS fragmentation functions [55]. The observed rise of the nuclear modification factor up to $R^*_{pPb} \approx 1.3$–1.4 at high p_T is stronger than expected theoretically. None of the available theoretical models [52] predict enhancements beyond $R_{pPb} \approx 1.1$ at high p_T. In particular, although the p_T range corresponds to parton momentum fractions $0.02 \lesssim x \lesssim 0.2$, which coincides with the region where parton antishadowing

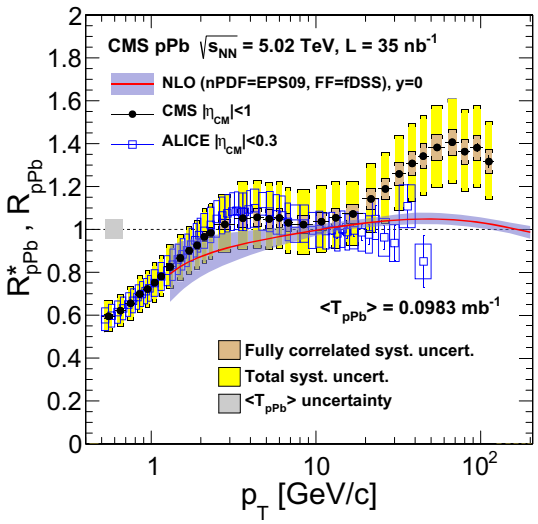

Fig. 5 Charged-particle nuclear modification factors measured by CMS in $|\eta_{CM}| < 1$ (*filled circles*), and by ALICE in $|\eta_{CM}| < 0.3$ (*open squares*), are compared to the NLO pQCD prediction of Ref. [53]. The theoretical uncertainty is based on the EPS09 error sets. For the CMS measurement, the *shaded band* at unity and $p_T \approx 0.6$ represents the uncertainty in the Glauber calculation of $\langle T_{pPb} \rangle$, the *smaller uncertainty band* around the data points shows the fully correlated uncertainties and the total systematic uncertainty is shown by the *larger band* (see Table 1). For the ALICE measurement, the total systematic uncertainties, excluding the normalization uncertainty of 6 %, are shown with *open boxes*

effects are expected [10], none of the nPDFs obtained from global fits to nuclear data predict enhancements beyond 10 % at the large virtualities ($Q^2 \sim p_T^2 \sim 500$–$10{,}000\ \mathrm{GeV}/c^2$) of relevance here.

An estimate of the significance of this observed rise above unity for $40 < p_T < 120\ \mathrm{GeV}/c$ is determined by interpreting all uncertainties as following a multivariate normal distribution where the components are the six p_T bins in the kinematic region of interest. The variance of each component is given by the sum of the statistical and systematic uncertainties in quadrature. For the case of the asymmetric particle species uncertainty, the smaller negative value is used as the data are uniformly larger than the expected values of the hypothesis to be tested. Given that the uncertainties of the reference spectrum are derived from applying different interpolation procedures and propagating the uncertainties from previous measurements from multiple experiments, it is not possible to unambiguously determine how all systematic uncertainties are correlated between measurements in each p_T bin. Therefore, a pair of estimates of the possible significance is given. In one case, only the systematic uncertainties from the relative normalization of the spectra, track selection, trigger efficiency, nuclear thickness function, and NLO pQCD calculation are treated as fully correlated, while others are treated as uncorrelated. In the other case, all systematic uncertainties are treated as fully correlated. Both the hypothesis that R^*_{pPb} is unity and the hypothesis that R^*_{pPb} is given by the NLO pQCD calculation are tested. For the case in which some uncertainties are treated as uncorrelated, a log-likelihood ratio test is performed using an alternative hypothesis that R^*_{pPb} is given by either unity or the NLO prediction, scaled by a constant, p_T-independent, factor. The hypothesis that R^*_{pPb} is unity for $40 < p_T < 120\ \mathrm{GeV}/c$ is rejected with a p value of 0.006 %, and the hypothesis that R^*_{pPb} is given by the NLO pQCD calculation for $40 < p_T < 120\ \mathrm{GeV}/c$ is rejected with a p value of 0.2 %. For the case in which all uncertainties are fully correlated, the log-likelihood ratio test cannot be used, as the covariance matrix becomes nearly singular and the maximum likelihood estimation fails. Instead, a two-tailed univariate test is performed using the single measurement for $61 < p_T < 74\ \mathrm{GeV}/c$. From this test, the hypothesis that R^*_{pPb} is unity for $61 < p_T < 74\ \mathrm{GeV}/c$ is rejected with a p value of 0.4 %, and the hypothesis that R^*_{pPb} is given by the NLO pQCD calculation for $61 < p_T < 74\ \mathrm{GeV}/c$ is rejected with a p value of 2 %.

Figure 5 also shows the measurement from the ALICE experiment [22], which is performed in a narrower pseudorapidity range than the CMS one, and uses a different method (NLO scaling) to obtain the pp reference spectrum based on ALICE pp data measured at $\sqrt{s} = 7$ TeV. The difference in the CMS and ALICE R^*_{pPb} results stems primarily from differences in the charged-hadron spectra measured in pp collisions at $\sqrt{s} = 7$ TeV [38,56].

Figure 6 shows the forward-backward yield asymmetry, Y_{asym} (Eq. 2), as a function of p_T for $0.3 < |\eta_{CM}| < 0.8$, $0.8 < |\eta_{CM}| < 1.3$, and $1.3 < |\eta_{CM}| < 1.8$. In all three η ranges, the value of Y_{asym} rises from $p_T \approx 0.4$ to about $3\ \mathrm{GeV}/c$, then falls to unity at a p_T of $10\ \mathrm{GeV}/c$, and remains constant at unity up to the highest p_T values. At the lowest p_T value, Y_{asym} is consistent with unity for $0.3 < |\eta_{CM}| < 0.8$, but is above unity in the larger pseudorapidity regions. For $p_T < 10\ \mathrm{GeV}/c$, the Y_{asym} is larger than unity as has been predicted by models including nuclear shadowing [52]. A theoretical NLO pQCD computation of Y_{asym} at high p_T [53], using CTEQ6 [57] free-proton PDFs, EPS09 nPDFs [4], and Kretzer parton-to-hadron fragmentation functions [58], is also shown in Fig. 6. The theoretical predictions are consistent with these data.

To determine if the R^*_{pPb} and Y_{asym} results can be consistently interpreted in terms of nPDF modifications, an MC study using the PYTHIA (Z2 tune) event generator was performed to correlate each high-p_T hadron to the fractional momentum, x, of the initial-state parton from the Pb nucleus that participated in the hard-scattering process producing the final hadron. In all pseudorapidity intervals studied here, most of the hadrons with $p_T \gtrsim 20\ \mathrm{GeV}/c$, i.e., in the range where the R^*_{pPb} exceeds unity in Fig. 4, come from the x region that is associated with antishadowing in the nPDF distributions. Although the mean of the x distribution increases

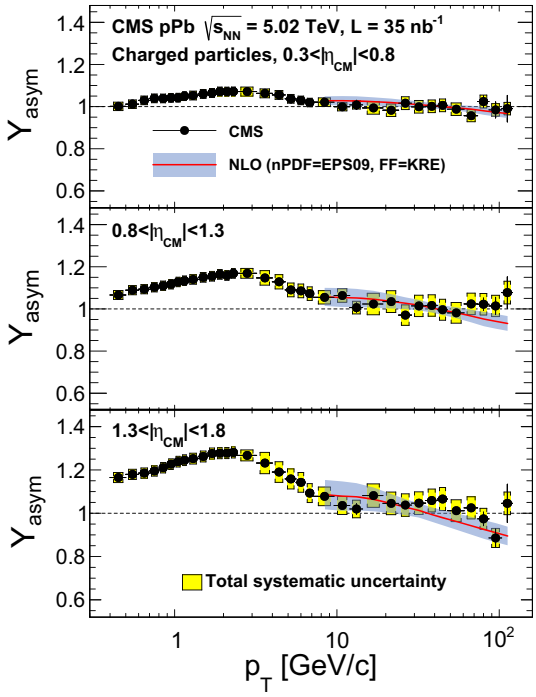

Fig. 6 Charged-particle forward-backward yield asymmetry as a function of p_T for $0.3 < |\eta_{CM}| < 0.8$ (*top*), $0.8 < |\eta_{CM}| < 1.3$ (*middle*), and $1.3 < |\eta_{CM}| < 1.8$ (*bottom*). The asymmetry is computed as the charged-particle yields in the direction of the Pb beam divided by those of the proton beam. The *solid curves* are NLO pQCD theoretical calculations including nPDFs modifications [53]. The theoretical uncertainty is based on the EPS09 error sets

with η_{CM}, for hadrons with p_T above 20 GeV/c it remains in the range $0.02 \lesssim x \lesssim 0.2$. Thus, similar antishadowing effects are expected in the positive and negative η_{CM} regions resulting in a Y_{asym} close to unity. At low p_T, corresponding to $x \lesssim 0.02$, a larger hadron yield is observed in the direction of the Pb beam. This is qualitatively consistent with expectations of gluon shadowing [52].

An enhancement in R^*_{pPb} at high p_T can possibly arise if the quark-jet fraction is larger in pPb than in pp collisions. Since the charged-particle products of quark fragmentation more often have higher relative p_T than those produced by gluon fragmentation, that could lead to an enhancement in the charged-particle production at high p_T beyond NLO expectations, without a corresponding increase in the jet R_{pPb} [25,26]. We note that the gluon-to-hadron fragmentation functions are not well constrained in pp collisions at LHC energies [27], although such uncertainties should largely cancel in ratios of cross sections.

5 Summary

Charged-particle spectra have been measured in pPb collisions at $\sqrt{s_{NN}} = 5.02$ TeV in the transverse momentum range of $0.4 < p_T < 120$ GeV/c for pseudorapidities up to $|\eta_{CM}| = 1.8$. The forward-backward yield asymmetry has been measured as a function of p_T for three bins in η_{CM}. At $p_T < 10$ GeV/c, the charged-particle production is enhanced in the direction of the Pb beam, in qualitative agreement with nuclear shadowing expectations. The nuclear modification factor at mid-rapidity, relative to a reference spectrum interpolated from pp measurements at lower and higher collision energies, rises above unity at high p_T reaching an R^*_{pPb} value of 1.3–1.4 at $p_T \gtrsim 40$ GeV/c. The observed enhancement is larger than expected from NLO pQCD predictions that include antishadowing effects in the nuclear PDFs in this kinematic range. Future direct measurement of the spectra of jets and charged particles in pp collisions at a center-of-mass energy of 5.02 TeV is necessary to better constrain the fragmentation functions and also to reduce the dominant systematic uncertainties in the charged-particle nuclear modification factor.

Acknowledgments We congratulate our colleagues in the CERN accelerator departments for the excellent performance of the LHC and thank the technical and administrative staffs at CERN and at other CMS institutes for their contributions to the success of the CMS effort. In addition, we gratefully acknowledge the computing centres and personnel of the Worldwide LHC Computing Grid for delivering so effectively the computing infrastructure essential to our analyses. Finally, we acknowledge the enduring support for the construction and operation of the LHC and the CMS detector provided by the following funding agencies: the Austrian Federal Ministry of Science, Research and Economy and the Austrian Science Fund; the Belgian Fonds de la Recherche Scientifique, and Fonds voor Wetenschappelijk Onderzoek; the Brazilian Funding Agencies (CNPq, CAPES, FAPERJ, and FAPESP); the Bulgarian Ministry of Education and Science; CERN; the Chinese Academy of Sciences, Ministry of Science and Technology, and National Natural Science Foundation of China; the Colombian Funding Agency (COLCIENCIAS); the Croatian Ministry of Science, Education and Sport, and the Croatian Science Foundation; the Research Promotion Foundation, Cyprus; the Ministry of Education and Research, Estonian Research Council via IUT23-4 and IUT23-6 and European Regional Development Fund, Estonia; the Academy of Finland, Finnish Ministry of Education and Culture, and Helsinki Institute of Physics; the Institut National de Physique Nucléaire et de Physique des Particules/CNRS, and Commissariat à l'Énergie Atomique et aux Énergies Alternatives/CEA, France; the Bundesministerium für Bildung und Forschung, Deutsche Forschungsgemeinschaft, and Helmholtz–Gemeinschaft Deutscher Forschungszentren, Germany; the General Secretariat for Research and Technology, Greece; the National Scientific Research Foundation, and National Innovation Office, Hungary; the Department of Atomic Energy and the Department of Science and Technology, India; the Institute for Studies in Theoretical Physics and Mathematics, Iran; the Science Foundation, Ireland; the Istituto Nazionale di Fisica Nucleare, Italy; the Ministry of Science, ICT and Future Planning, and National Research Foundation (NRF), Republic of Korea; the Lithuanian Academy of Sciences; the Ministry of Education, and University of Malaya (Malaysia); the Mexican Funding Agencies (CINVESTAV, CONACYT, SEP, and UASLP-FAI); the Ministry of Business, Innovation and Employment, New Zealand; the Pakistan Atomic Energy Commission; the Ministry of Science and Higher Education and the National Science Centre, Poland; the Fundação para a Ciência e a Tecnologia, Portugal; JINR, Dubna; the Ministry of Education and Science of the Russian Federation, the Federal Agency of

Atomic Energy of the Russian Federation, Russian Academy of Sciences, and the Russian Foundation for Basic Research; the Ministry of Education, Science and Technological Development of Serbia; the Secretaría de Estado de Investigación, Desarrollo e Innovación and Programa Consolider-Ingenio 2010, Spain; the Swiss Funding Agencies (ETH Board, ETH Zurich, PSI, SNF, UniZH, Canton Zurich, and SER); the Ministry of Science and Technology, Taipei; the Thailand Center of Excellence in Physics, the Institute for the Promotion of Teaching Science and Technology of Thailand, Special Task Force for Activating Research and the National Science and Technology Development Agency of Thailand; the Scientific and Technical Research Council of Turkey, and Turkish Atomic Energy Authority; the National Academy of Sciences of Ukraine, and State Fund for Fundamental Researches, Ukraine; the Science and Technology Facilities Council, UK; the US Department of Energy, and the US National Science Foundation. Individuals have received support from the Marie-Curie programme and the European Research Council and EPLANET (European Union); the Leventis Foundation; the A. P. Sloan Foundation; the Alexander von Humboldt Foundation; the Belgian Federal Science Policy Office; the Fonds pour la Formation à la Recherche dans l'Industrie et dans l'Agriculture (FRIA-Belgium); the Agentschap voor Innovatie door Wetenschap en Technologie (IWT-Belgium); the Ministry of Education, Youth and Sports (MEYS) of the Czech Republic; the Council of Science and Industrial Research, India; the HOMING PLUS programme of Foundation for Polish Science, cofinanced from European Union, Regional Development Fund; the Compagnia di San Paolo (Torino); the Consorzio per la Fisica (Trieste); MIUR project 20108T4XTM (Italy); the Thalis and Aristeia programmes cofinanced by EU-ESF and the Greek NSRF; and the National Priorities Research Program by Qatar National Research Fund.

References

1. J.D. Bjorken, Energy loss of energetic partons in quark–gluon plasma: possible extinction of high p(t) jets in hadron–hadron collisions. Technical Report FERMILAB-PUB-82-059-T, Fermilab (1982)
2. D. d'Enterria, "6.4 Jet quenching", Springer materials—the Landolt–Börnstein. Database **23**, 471 (2010). doi:10.1007/978-3-642-01539-7_16. arXiv:0902.2011
3. M.L. Miller, K. Reygers, S.J. Sanders, P. Steinberg, Glauber modeling in high energy nuclear collisions. Ann. Rev. Nucl. Part. Sci. **57**, 205 (2007). doi:10.1146/annurev.nucl.57.090506.123020
4. K.J. Eskola, H. Paukkunen, C.A. Salgado, EPS09: a new generation of NLO and LO nuclear parton distribution functions. JHEP **04**, 065 (2009). doi:10.1088/1126-6708/2009/04/065. arXiv:0902.4154
5. M. Arneodo, Nuclear effects in structure functions. Phys. Rep. **240**, 301 (1994). doi:10.1016/0370-1573(94)90048-5
6. L.L. Frankfurt, M.I. Strikman, Hard nuclear processes and microscopic nuclear structure. Phys. Rep. **160**, 235 (1988). doi:10.1016/0370-1573(88)90179-2
7. E. Iancu, L.D. McLerran, Saturation and universality in QCD at small x. Phys. Lett. B **510**, 145 (2001). doi:10.1016/S0370-2693(01)00526-3. arXiv:hep-ph/0103032
8. E. Iancu, R. Venugopalan, The color glass condensate and high energy scattering in QCD. in *Quark–Gluon Plasma*, vol. 3. ed by R.C. Hwa, W.X.-N (World Scientific, Singapore, 2003), p. 249. arXiv:hep-ph/0303204
9. J.L. Albacete, A. Dumitru, C. Marquet, The initial state of heavy-ion collisions. Int. J. Mod. Phys. A **28**, 1340010 (2013). doi:10.1142/S0217751X13400101. arXiv:1302.6433
10. C.A. Salgado et al., Proton–nucleus collisions at the LHC: scientific opportunities and requirements. J. Phys. G **39**, 015010 (2012). doi:10.1088/0954-3899/39/1/015010. arXiv:1105.3919
11. PHENIX Collaboration, Suppressed π^0 production at large transverse momentum in central Au+Au collisions at $\sqrt{s_{\rm NN}}$ = 200 GeV. Phys. Rev. Lett. **91**, 072301 (2003). doi:10.1103/PhysRevLett.91.072301. arXiv:nucl-ex/0304022
12. PHENIX Collaboration, High-$p_{\rm T}$ charged hadron suppression in Au + Au collisions at $\sqrt{s_{\rm NN}}$ = 200 GeV. Phys. Rev. C **69**, 034910 (2004). doi:10.1103/PhysRevC.69.034910. arXiv:nucl-ex/0308006
13. PHOBOS Collaboration, Charged hadron transverse momentum distributions in Au + Au collisions at $\sqrt{s_{\rm NN}}$ = 200 GeV. Phys. Lett. B **578**, 297 (2004). doi:10.1016/j.physletb.2003.10.101. arXiv:nucl-ex/0302015
14. STAR Collaboration, Transverse-momentum and collision-energy dependence of high-$p_{\rm T}$ hadron suppression in Au+Au collisions at ultrarelativistic energies. Phys. Rev. Lett. **91**, 172302 (2003). doi:10.1103/PhysRevLett.91.172302. arXiv:nucl-ex/0305015
15. BRAHMS Collaboration, Transverse momentum spectra in Au+Au and d+Au collisions at $\sqrt{s_{\rm NN}}$ = 200 GeV and the pseudorapidity dependence of high-$p_{\rm t}$ suppression. Phys. Rev. Lett. **91**, 072305 (2003). doi:10.1103/PhysRevLett.91.072305. arXiv:nucl-ex/0307003
16. PHENIX Collaboration, Absence of suppression in particle production at large transverse momentum in $\sqrt{s_{\rm NN}}$ = 200 GeV d+Au collisions. Phys. Rev. Lett. **91**, 072303 (2003). doi:10.1103/PhysRevLett.91.072303. arXiv:nucl-ex/0306021
17. PHOBOS Collaboration, Centrality dependence of charged-hadron transverse-momentum spectra in d+Au collisions at $\sqrt{s_{\rm NN}}$ = 200 GeV. Phys. Rev. Lett. **91**, 072302 (2003). doi:10.1103/PhysRevLett.91.072302. arXiv:nucl-ex/0306025
18. STAR Collaboration, Evidence from d+Au measurements for final-state suppression of high-$p_{\rm T}$ hadrons in Au+Au collisions at RHIC. Phys. Rev. Lett. **91**, 072304 (2003). doi:10.1103/PhysRevLett.91.072304. arXiv:nucl-ex/0306024
19. D. Kharzeev, E. Levin, L. McLerran, Parton saturation and $N_{\rm part}$ scaling of semi-hard processes in QCD. Phys. Lett. B **561**, 93 (2003). doi:10.1016/S0370-2693(03)00420-9. arXiv:hep-ph/0210332
20. CMS Collaboration, Study of high-p_T charged particle suppression in PbPb compared to pp collisions at $\sqrt{s_{NN}}$=2.76 TeV. Eur. Phys. J. C **72**, 1945 (2012). doi:10.1140/epjc/s10052-012-1945-x. arXiv:1202.2554
21. ALICE Collaboration, Centrality dependence of charged particle production at large transverse momentum in Pb–Pb collisions at $\sqrt{s_{\rm NN}}$ = 2.76 TeV. Phys. Lett. B **720**, 52 (2013). doi:10.1016/j.physletb.2013.01.051. arXiv:1208.2711
22. ALICE Collaboration, Transverse momentum dependence of inclusive primary charged-particle production in p-Pb collisions at $\sqrt{s_{\rm NN}}$ = 5.02TeV. Eur. Phys. J. C **74**, 3054 (2014). doi:10.1140/epjc/s10052-014-3054-5. arXiv:1405.2737
23. CMS Collaboration, Studies of dijet transverse momentum balance and pseudorapidity distributions in pPb collisions at $\sqrt{s_{\rm NN}}$ = 5.02 TeV. Eur. Phys. J. C **74**, 2951 (2014). doi:10.1140/epjc/s10052-014-2951-y. arXiv:1401.4433
24. I. Helenius, K.J. Eskola, H. Honkanen, C.A. Salgado, Impact-parameter dependent nuclear parton distribution functions: EPS09s and EKS98s and their applications in nuclear hard processes. JHEP **07**, 073 (2012). doi:10.1007/JHEP07(2012)073. arXiv:1205.5359

25. ATLAS Collaboration, Measurements of the nuclear modification factor for jets in Pb+Pb collisions at $\sqrt{s_{\rm NN}}$ = 2.76 TeV with the ATLAS detector. Phys. Rev. Lett. **114**, 072302 (2015). doi:10.1103/PhysRevLett.114.072302. arXiv:1411.2357
26. ALICE Collaboration, Measurement of charged jet production cross sections and nuclear modification in p-Pb collisions at $\sqrt{s_{\rm NN}}$ = 5.02 TeV. Phys. Lett. B (2015, submitted). arXiv:1503.00681
27. D. d'Enterria, K.J. Eskola, I. Helenius, H. Paukkunen, Confronting current NLO parton fragmentation functions with inclusive charged-particle spectra at hadron colliders. Nucl. Phys. B **883**, 615 (2014). doi:10.1016/j.nuclphysb.2014.04.006. arXiv:1311.1415
28. CMS Collaboration, The CMS experiment at the CERN LHC. JINST **3**, S08004 (2008). doi:10.1088/1748-0221/3/08/S08004
29. GEANT4 Collaboration, GEANT4–a simulation toolkit. Nucl. Instrum. Meth. A **506**, 250 (2003). doi:10.1016/S0168-9002(03)01368-8
30. CMS Collaboration, CMS tracking performance results from early LHC operation. Eur. Phys. J. C **70**, 1165 (2010). doi:10.1140/epjc/s10052-010-1491-3. arXiv:1007.1988
31. CMS Collaboration, Study of the production of charged pions, kaons, and protons in pPb collisions at $\sqrt{s_{\rm NN}}$ = 5.02 TeV. Eur. Phys. J. C **74**, 2847 (2014). doi:10.1140/epjc/s10052-014-2847-x. arXiv:1307.3442
32. X.-N. Wang, M. Gyulassy, HIJING: a monte carlo model for multiple jet production in pp, pA and AA collisions. Phys. Rev. D **44**, 3501 (1991). doi:10.1103/PhysRevD.44.3501
33. M. Gyulassy, X.-N. Wang, HIJING 1.0: a monte carlo program for parton and particle production in high-energy hadronic and nuclear collisions. Comput. Phys. Commun. **83**, 307 (1994). doi:10.1016/0010-4655(94)90057-4. arXiv:nucl-th/9502021
34. K. Werner, F.-M. Liu, T. Pierog, Parton ladder splitting and the rapidity dependence of transverse momentum spectra in deuteron–gold collisions at RHIC. Phys. Rev. C **74**, 044902 (2006). doi:10.1103/PhysRevC.74.044902. arXiv:hep-ph/0506232
35. CMS Collaboration, Description and performance of track and primary-vertex reconstruction with the CMS tracker. JINST **9**, P10009 (2014). doi:10.1088/1748-0221/9/10/P10009. arXiv:1405.6569
36. T. Sjöstrand, S. Mrenna, P. Skands, PYTHIA 6.4 physics and manual. JHEP **05**, 026 (2006). doi:10.1088/1126-6708/2006/05/026. arXiv:hep-ph/0603175
37. R. Field, Early LHC underlying event data—findings and surprises. in *22nd Hadron Collider Physics Symposium (HCP 2010)*, ed. by W. Trischuk (Toronto, 2010). arXiv:1010.3558
38. CMS Collaboration, Charged particle transverse momentum spectra in pp collisions at $\sqrt{s}$ = 0.9 and 7 Te V. JHEP **08**, 086 (2011). doi:10.1007/JHEP08(2011)086. arXiv:1104.3547
39. CDF Collaboration, Transverse momentum distributions of charged particles produced interactions at $\sqrt{s}$ = 630 GeV and 1800 GeV. Phys. Rev. Lett. **61**, 1819 (1988). doi:10.1103/PhysRevLett.61.1819
40. CDF Collaboration, Erratum: measurement of particle production and inclusive differential cross sections in $p\bar{p}$ collisions at $\sqrt{s}$ = 1.96 TeV [Phys. Rev. D 79, 112005]. Phys. Rev. D **82**(2010), 119903 (2009). doi:10.1103/PhysRevD.82.119903
41. F. Arleo, D. d'Enterria, A.S. Yoon, Single-inclusive production of large-$p_{\rm T}$ charged particles in hadronic collisions at TeV energies and perturbative QCD predictions. JHEP **06**, 035 (2010). doi:10.1007/JHEP06(2010)035. arXiv:1003.2963
42. B. Alver, M. Baker, C. Loizides, P. Steinberg, The PHOBOS Glauber Monte Carlo (2008). arXiv:0805.4411
43. H. De Vries, C.W. De Jager, C. De Vries, Nuclear charge and magnetization density distribution parameters from elastic electron scattering. Atom. Data Nucl. Data Tabl. **36**, 495 (1987). doi:10.1016/0092-640X(87)90013-1
44. J.W. Cronin et al., Production of hadrons at large transverse momentum at 200, 300, and 400 GeV. Phys. Rev. D **11**, 3105 (1975). doi:10.1103/PhysRevD.11.3105
45. R.C. Hwa, Hadron correlations in jets and ridges through parton recombination. in *Quark–Gluon Plasma*, vol. 4, ed. by R.C. Hwa (World Scientific, Singapore, 2010), p. 249. arXiv:0904.2159
46. CMS Collaboration, Observation of long-range near-side angular correlations in proton–lead collisions at the LHC. Phys. Lett. B **718**, 795 (2013). doi:10.1016/j.physletb.2012.11.025. arXiv:1210.5482
47. ALICE Collaboration, Long-range angular correlations on the near and away side in p-Pb collisions at $\sqrt{s_{\rm NN}}$ = 5.02 TeV. Phys. Lett. B **719**, 29 (2013). doi:10.1016/j.physletb.2013.01.012. arXiv:1212.2001
48. ATLAS Collaboration, Observation of associated near-side and away-side long-range correlations in $\sqrt{s_{\rm NN}}$ = 5.02 TeV proton–lead collisions with the ATLAS detector. Phys. Rev. Lett. **110**, 182302 (2013). doi:10.1103/PhysRevLett.110.182302. arXiv:1212.5198
49. CMS Collaboration, Multiplicity and transverse momentum dependence of two- and four-particle correlations in pPb and PbPb collisions. Phys. Lett. B **724**, 213 (2013). doi:10.1016/j.physletb.2013.06.028. arXiv:1305.0609
50. PHENIX Collaboration, Spectra and ratios of identified particles in Au+Au and d+Au collisions at $\sqrt{s_{\rm NN}}$ = 200 GeV. Phys. Rev. C **88**, 024906 (2013). doi:10.1103/PhysRevC.88.024906. arXiv:1304.3410
51. PHENIX Collaboration, Measurement of long-range angular correlation and quadrupole anisotropy of pions and (anti)protons in central d+Au collisions at $\sqrt{s_{\rm NN}}$ = 200 GeV. Phys. Rev. Lett. 114, 192301 (2015). doi:10.1103/PhysRevLett.114.192301
52. J.L. Albacete et al., Predictions for p+Pb collisions at $\sqrt{s_{\rm NN}}$ = 5 TeV. Int. J. Mod. Phys. E **22**, 1330007 (2013). doi:10.1142/S0218301313300075. arXiv:1301.3395
53. H. Paukkunen, The LHC p+Pb run from the nuclear PDF perspective. In: XXII. Int. Workshop on Deep-Inelastice Scattering and Related Subjects, p. 053. Warsaw, Poland (2014). arXiv:1408.4657. PoS(DIS2014)053
54. H.-L. Lai et al., New parton distributions for collider physics. Phys. Rev. D **82**, 074024 (2010). doi:10.1103/PhysRevD.82.074024. arXiv:1007.2241
55. D. de Florian, R. Sassot, M. Stratmann, Global analysis of fragmentation functions for pions and kaons and their uncertainties. Phys. Rev. D **75**, 114010 (2007). doi:10.1103/PhysRevD.75.114010. arXiv:hep-ph/0703242
56. ALICE Collaboration, Energy dependence of the transverse momentum distributions of charged particles in pp collisions measured by ALICE. Eur. Phys. J. C **73**, 2662 (2013). doi:10.1140/epjc/s10052-013-2662-9. arXiv:1307.1093
57. P.M. Nadolsky et al., Implications of CTEQ global analysis for collider observables. Phys. Rev. D **78**, 013004 (2008). doi:10.1103/PhysRevD.78.013004. arXiv:0802.0007
58. S. Kretzer, Fragmentation functions from flavor inclusive and flavor tagged e+ e− annihilations. Phys. Rev. D **62**, 054001 (2000). doi:10.1103/PhysRevD.62.054001. arXiv:hep-ph/0003177

CMS Collaboration

Yerevan Physics Institute, Yerevan, Armenia
V. Khachatryan, A. M. Sirunyan, A. Tumasyan

Institut für Hochenergiephysik der OeAW, Wien, Austria
W. Adam, T. Bergauer, M. Dragicevic, J. Erö, M. Friedl, R. Frühwirth[1], V. M. Ghete, C. Hartl, N. Hörmann, J. Hrubec, M. Jeitler[1], W. Kiesenhofer, V. Knünz, M. Krammer[1], I. Krätschmer, D. Liko, I. Mikulec, D. Rabady[2], B. Rahbaran, H. Rohringer, R. Schöfbeck, J. Strauss, W. Treberer-Treberspurg, W. Waltenberger, C.-E. Wulz[1]

National Centre for Particle and High Energy Physics, Minsk, Belarus
V. Mossolov, N. Shumeiko, J. Suarez Gonzalez

Universiteit Antwerpen, Antwerpen, Belgium
S. Alderweireldt, S. Bansal, T. Cornelis, E. A. De Wolf, X. Janssen, A. Knutsson, J. Lauwers, S. Luyckx, S. Ochesanu, R. Rougny, M. Van De Klundert, H. Van Haevermaet, P. Van Mechelen, N. Van Remortel, A. Van Spilbeeck

Vrije Universiteit Brussel, Brussels, Belgium
F. Blekman, S. Blyweert, J. D'Hondt, N. Daci, N. Heracleous, J. Keaveney, S. Lowette, M. Maes, A. Olbrechts, Q. Python, D. Strom, S. Tavernier, W. Van Doninck, P. Van Mulders, G. P. Van Onsem, I. Villella

Université Libre de Bruxelles, Bruxelles, Belgium
C. Caillol, B. Clerbaux, G. De Lentdecker, D. Dobur, L. Favart, A. P. R. Gay, A. Grebenyuk, A. Léonard, A. Mohammadi, L. Perniè[2], A. Randle-conde, T. Reis, T. Seva, L. Thomas, C. Vander Velde, P. Vanlaer, J. Wang, F. Zenoni

Ghent University, Ghent, Belgium
V. Adler, K. Beernaert, L. Benucci, A. Cimmino, S. Costantini, S. Crucy, S. Dildick, A. Fagot, G. Garcia, J. Mccartin, A. A. Ocampo Rios, D. Ryckbosch, S. Salva Diblen, M. Sigamani, N. Strobbe, F. Thyssen, M. Tytgat, E. Yazgan, N. Zaganidis

Université Catholique de Louvain, Louvain-la-Neuve, Belgium
S. Basegmez, C. Beluffi[3], G. Bruno, R. Castello, A. Caudron, L. Ceard, G. G. Da Silveira, C. Delaere, T. du Pree, D. Favart, L. Forthomme, A. Giammanco[4], J. Hollar, A. Jafari, P. Jez, M. Komm, V. Lemaitre, C. Nuttens, D. Pagano, L. Perrini, A. Pin, K. Piotrzkowski, A. Popov[5], L. Quertenmont, M. Selvaggi, M. Vidal Marono, J. M. Vizan Garcia

Université de Mons, Mons, Belgium
N. Beliy, T. Caebergs, E. Daubie, G. H. Hammad

Centro Brasileiro de Pesquisas Fisicas, Rio de Janeiro, Brazil
W. L. Aldá Júnior, G. A. Alves, L. Brito, M. Correa Martins Junior, T. Dos Reis Martins, C. Mora Herrera, M. E. Pol

Universidade do Estado do Rio de Janeiro, Rio de Janeiro, Brazil
W. Carvalho, J. Chinellato[6], A. Custódio, E. M. Da Costa, D. De Jesus Damiao, C. De Oliveira Martins, S. Fonseca De Souza, H. Malbouisson, D. Matos Figueiredo, L. Mundim, H. Nogima, W. L. Prado Da Silva, J. Santaolalla, A. Santoro, A. Sznajder, E. J. Tonelli Manganote[6], A. Vilela Pereira

Universidade Estadual Paulista[a], Universidade Federal do ABC[b], São Paulo, Brazil
C. A. Bernardes[b], S. Dogra[a], T. R. Fernandez Perez Tomei[a], E. M. Gregores[b], P. G. Mercadante[b], S. F. Novaes[a], Sandra S. Padula[a]

Institute for Nuclear Research and Nuclear Energy, Sofia, Bulgaria
A. Aleksandrov, V. Genchev[2], R. Hadjiiska, P. Iaydjiev, A. Marinov, S. Piperov, M. Rodozov, G. Sultanov, M. Vutova

University of Sofia, Sofia, Bulgaria
A. Dimitrov, I. Glushkov, L. Litov, B. Pavlov, P. Petkov

Institute of High Energy Physics, Beijing, China
J. G. Bian, G. M. Chen, H. S. Chen, M. Chen, T. Cheng, R. Du, C. H. Jiang, R. Plestina[7], F. Romeo, J. Tao, Z. Wang

State Key Laboratory of Nuclear Physics and Technology, Peking University, Beijing, China
C. Asawatangtrakuldee, Y. Ban, S. Liu, Y. Mao, S. J. Qian, D. Wang, Z. Xu, L. Zhang, W. Zou

Universidad de Los Andes, Bogota, Colombia
C. Avila, A. Cabrera, L. F. Chaparro Sierra, C. Florez, J. P. Gomez, B. Gomez Moreno, J. C. Sanabria

Faculty of Electrical Engineering, Mechanical Engineering and Naval Architecture, University of Split, Split, Croatia
N. Godinovic, D. Lelas, D. Polic, I. Puljak

Faculty of Science, University of Split, Split, Croatia
Z. Antunovic, M. Kovac

Institute Rudjer Boskovic, Zagreb, Croatia
V. Brigljevic, K. Kadija, J. Luetic, D. Mekterovic, L. Sudic

University of Cyprus, Nicosia, Cyprus
A. Attikis, G. Mavromanolakis, J. Mousa, C. Nicolaou, F. Ptochos, P. A. Razis

Charles University, Prague, Czech Republic
M. Bodlak, M. Finger, M. Finger Jr.[8]

Academy of Scientific Research and Technology of the Arab Republic of Egypt, Egyptian Network of High Energy Physics, Cairo, Egypt
Y. Assran[9], A. Ellithi Kamel[10], M. A. Mahmoud[11], A. Radi[12,13]

National Institute of Chemical Physics and Biophysics, Tallinn, Estonia
M. Kadastik, M. Murumaa, M. Raidal, A. Tiko

Department of Physics, University of Helsinki, Helsinki, Finland
P. Eerola, G. Fedi, M. Voutilainen

Helsinki Institute of Physics, Helsinki, Finland
J. Härkönen, V. Karimäki, R. Kinnunen, M. J. Kortelainen, T. Lampén, K. Lassila-Perini, S. Lehti, T. Lindén, P. Luukka, T. Mäenpää, T. Peltola, E. Tuominen, J. Tuominiemi, E. Tuovinen, L. Wendland

Lappeenranta University of Technology, Lappeenranta, Finland
J. Talvitie, T. Tuuva

DSM/IRFU, CEA/Saclay, Gif-sur-Yvette, France
M. Besancon, F. Couderc, M. Dejardin, D. Denegri, B. Fabbro, J. L. Faure, C. Favaro, F. Ferri, S. Ganjour, A. Givernaud, P. Gras, G. Hamel de Monchenault, P. Jarry, E. Locci, J. Malcles, J. Rander, A. Rosowsky, M. Titov

Laboratoire Leprince-Ringuet, Ecole Polytechnique, IN2P3-CNRS, Palaiseau, France
S. Baffioni, F. Beaudette, P. Busson, C. Charlot, T. Dahms, M. Dalchenko, L. Dobrzynski, N. Filipovic, A. Florent, R. Granier de Cassagnac, L. Mastrolorenzo, P. Miné, C. Mironov, I. N. Naranjo, M. Nguyen, C. Ochando, P. Paganini, S. Regnard, R. Salerno, J. B. Sauvan, Y. Sirois, C. Veelken, Y. Yilmaz, A. Zabi

Institut Pluridisciplinaire Hubert Curien, Université de Strasbourg, Université de Haute Alsace Mulhouse, CNRS/IN2P3, Strasbourg, France
J.-L. Agram[14], J. Andrea, A. Aubin, D. Bloch, J.-M. Brom, E. C. Chabert, C. Collard, E. Conte[14], J.-C. Fontaine[14], D. Gelé, U. Goerlach, C. Goetzmann, A.-C. Le Bihan, K. Skovpen, P. Van Hove

Centre de Calcul de l'Institut National de Physique Nucleaire et de Physique des Particules, CNRS/IN2P3, Villeurbanne, France
S. Gadrat

Institut de Physique Nucléaire de Lyon, Université de Lyon, Université Claude Bernard Lyon 1, CNRS-IN2P3, Villeurbanne, France
S. Beauceron, N. Beaupere, G. Boudoul[2], E. Bouvier, S. Brochet, C. A. Carrillo Montoya, J. Chasserat, R. Chierici, D. Contardo[2], P. Depasse, H. El Mamouni, J. Fan, J. Fay, S. Gascon, M. Gouzevitch, B. Ille, T. Kurca, M. Lethuillier,

L. Mirabito, S. Perries, J. D. Ruiz Alvarez, D. Sabes, L. Sgandurra, V. Sordini, M. Vander Donckt, P. Verdier, S. Viret, H. Xiao

Institute of High Energy Physics and Informatization, Tbilisi State University, Tbilisi, Georgia
Z. Tsamalaidze[8]

I. Physikalisches Institut, RWTH Aachen University, Aachen, Germany
C. Autermann, S. Beranek, M. Bontenackels, M. Edelhoff, L. Feld, A. Heister, O. Hindrichs, K. Klein, A. Ostapchuk, F. Raupach, J. Sammet, S. Schael, J. F. Schulte, H. Weber, B. Wittmer, V. Zhukov[5]

III. Physikalisches Institut A, RWTH Aachen University, Aachen, Germany
M. Ata, M. Brodski, E. Dietz-Laursonn, D. Duchardt, M. Erdmann, R. Fischer, A. Güth, T. Hebbeker, C. Heidemann, K. Hoepfner, D. Klingebiel, S. Knutzen, P. Kreuzer, M. Merschmeyer, A. Meyer, P. Millet, M. Olschewski, K. Padeken, P. Papacz, H. Reithler, S. A. Schmitz, L. Sonnenschein, D. Teyssier, S. Thüer, M. Weber

III. Physikalisches Institut B, RWTH Aachen University, Aachen, Germany
V. Cherepanov, Y. Erdogan, G. Flügge, H. Geenen, M. Geisler, W. Haj Ahmad, F. Hoehle, B. Kargoll, T. Kress, Y. Kuessel, A. Künsken, J. Lingemann[2], A. Nowack, I. M. Nugent, L. Perchalla, O. Pooth, A. Stahl

Deutsches Elektronen-Synchrotron, Hamburg, Germany
M. Aldaya Martin, I. Asin, N. Bartosik, J. Behr, U. Behrens, A. J. Bell, A. Bethani, K. Borras, A. Burgmeier, A. Cakir, L. Calligaris, A. Campbell, S. Choudhury, F. Costanza, C. Diez Pardos, G. Dolinska, S. Dooling, T. Dorland, G. Eckerlin, D. Eckstein, T. Eichhorn, G. Flucke, J. Garay Garcia, A. Geiser, P. Gunnellini, J. Hauk, M. Hempel[15], H. Jung, A. Kalogeropoulos, M. Kasemann, P. Katsas, J. Kieseler, C. Kleinwort, I. Korol, D. Krücker, W. Lange, J. Leonard, K. Lipka, A. Lobanov, W. Lohmann[15], B. Lutz, R. Mankel, I. Marfin[15], I.-A. Melzer-Pellmann, A. B. Meyer, G. Mittag, J. Mnich, A. Mussgiller, S. Naumann-Emme, A. Nayak, E. Ntomari, H. Perrey, D. Pitzl, R. Placakyte, A. Raspereza, P. M. Ribeiro Cipriano, B. Roland, E. Ron, M. Ö. Sahin, J. Salfeld-Nebgen, P. Saxena, T. Schoerner-Sadenius, M. Schröder, C. Seitz, S. Spannagel, A. D. R. Vargas Trevino, R. Walsh, C. Wissing

University of Hamburg, Hamburg, Germany
V. Blobel, M. Centis Vignali, A. R. Draeger, J. Erfle, E. Garutti, K. Goebel, M. Görner, J. Haller, M. Hoffmann, R. S. Höing, A. Junkes, H. Kirschenmann, R. Klanner, R. Kogler, J. Lange, T. Lapsien, T. Lenz, I. Marchesini, J. Ott, T. Peiffer, A. Perieanu, N. Pietsch, J. Poehlsen, T. Poehlsen, D. Rathjens, C. Sander, H. Schettler, P. Schleper, E. Schlieckau, A. Schmidt, M. Seidel, V. Sola, H. Stadie, G. Steinbrück, D. Troendle, E. Usai, L. Vanelderen, A. Vanhoefer

Institut für Experimentelle Kernphysik, Karlsruhe, Germany
C. Barth, C. Baus, J. Berger, C. Böser, E. Butz, T. Chwalek, W. De Boer, A. Descroix, A. Dierlamm, M. Feindt, F. Frensch, M. Giffels, A. Gilbert, F. Hartmann[2], T. Hauth, U. Husemann, I. Katkov[5], A. Kornmayer[2], E. Kuznetsova, P. Lobelle Pardo, M. U. Mozer, T. Müller, Th. Müller, A. Nürnberg, G. Quast, K. Rabbertz, S. Röcker, H. J. Simonis, F. M. Stober, R. Ulrich, J. Wagner-Kuhr, S. Wayand, T. Weiler, R. Wolf

Institute of Nuclear and Particle Physics (INPP), NCSR Demokritos, Aghia Paraskevi, Greece
G. Anagnostou, G. Daskalakis, T. Geralis, V. A. Giakoumopoulou, A. Kyriakis, D. Loukas, A. Markou, C. Markou, A. Psallidas, I. Topsis-Giotis

University of Athens, Athens, Greece
A. Agapitos, S. Kesisoglou, A. Panagiotou, N. Saoulidou, E. Stiliaris

University of Ioánnina, Ioánnina, Greece
X. Aslanoglou, I. Evangelou, G. Flouris, C. Foudas, P. Kokkas, N. Manthos, I. Papadopoulos, E. Paradas, J. Strologas

Wigner Research Centre for Physics, Budapest, Hungary
G. Bencze, C. Hajdu, P. Hidas, D. Horvath[16], F. Sikler, V. Veszpremi, G. Vesztergombi[17], A. J. Zsigmond

Institute of Nuclear Research ATOMKI, Debrecen, Hungary
N. Beni, S. Czellar, J. Karancsi[18], J. Molnar, J. Palinkas, Z. Szillasi

University of Debrecen, Debrecen, Hungary
A. Makovec, P. Raics, Z. L. Trocsanyi, B. Ujvari

National Institute of Science Education and Research, Bhubaneswar, India
S. K. Swain

Panjab University, Chandigarh, India
S. B. Beri, V. Bhatnagar, R. Gupta, U. Bhawandeep, A. K. Kalsi, M. Kaur, R. Kumar, M. Mittal, N. Nishu, J. B. Singh

University of Delhi, Delhi, India
Ashok Kumar, Arun Kumar, S. Ahuja, A. Bhardwaj, B. C. Choudhary, A. Kumar, S. Malhotra, M. Naimuddin, K. Ranjan, V. Sharma

Saha Institute of Nuclear Physics, Kolkata, India
S. Banerjee, S. Bhattacharya, K. Chatterjee, S. Dutta, B. Gomber, Sa. Jain, Sh. Jain, R. Khurana, A. Modak, S. Mukherjee, D. Roy, S. Sarkar, M. Sharan

Bhabha Atomic Research Centre, Mumbai, India
A. Abdulsalam, D. Dutta, S. Kailas, V. Kumar, A. K. Mohanty[2], L. M. Pant, P. Shukla, A. Topkar

Tata Institute of Fundamental Research, Mumbai, India
T. Aziz, S. Banerjee, S. Bhowmik[19], R. M. Chatterjee, R. K. Dewanjee, S. Dugad, S. Ganguly, S. Ghosh, M. Guchait, A. Gurtu[20], G. Kole, S. Kumar, M. Maity[19], G. Majumder, K. Mazumdar, G. B. Mohanty, B. Parida, K. Sudhakar, N. Wickramage[21]

Institute for Research in Fundamental Sciences (IPM), Tehran, Iran
H. Bakhshiansohi, H. Behnamian, S. M. Etesami[22], A. Fahim[23], R. Goldouzian, M. Khakzad, M. Mohammadi Najafabadi, M. Naseri, S. Paktinat Mehdiabadi, F. Rezaei Hosseinabadi, B. Safarzadeh[24], M. Zeinali

University College Dublin, Dublin, Ireland
M. Felcini, M. Grunewald

INFN Sezione di Bari[a], Università di Bari[b], Politecnico di Bari[c], Bari, Italy
M. Abbrescia[a,b], C. Calabria[a,b], S. S. Chhibra[a,b], A. Colaleo[a], D. Creanza[a,c], N. De Filippis[a,c], M. De Palma[a,b], L. Fiore[a], G. Iaselli[a,c], G. Maggi[a,c], M. Maggi[a], S. My[a,c], S. Nuzzo[a,b], A. Pompili[a,b], G. Pugliese[a,c], R. Radogna[a,b,2], G. Selvaggi[a,b], A. Sharma, L. Silvestris[a,2], R. Venditti[a,b], P. Verwilligen[a]

INFN Sezione di Bologna[a], Università di Bologna[b], Bologna, Italy
G. Abbiendi[a], A. C. Benvenuti[a], D. Bonacorsi[a,b], S. Braibant-Giacomelli[a,b], L. Brigliadori[a,b], R. Campanini[a,b], P. Capiluppi[a,b], A. Castro[a,b], F. R. Cavallo[a], G. Codispoti[a,b], M. Cuffiani[a,b], G. M. Dallavalle[a], F. Fabbri[a], A. Fanfani[a,b], D. Fasanella[a,b], P. Giacomelli[a], C. Grandi[a], L. Guiducci[a,b], S. Marcellini[a], G. Masetti[a], A. Montanari[a], F. L. Navarria[a,b], A. Perrotta[a], F. Primavera[a,b], A. M. Rossi[a,b], T. Rovelli[a,b], G. P. Siroli[a,b], N. Tosi[a,b], R. Travaglini[a,b]

INFN Sezione di Catania[a], Università di Catania[b], CSFNSM[c], Catania, Italy
S. Albergo[a,b], G. Cappello[a], M. Chiorboli[a,b], S. Costa[a,b], F. Giordano[a,2], R. Potenza[a,b], A. Tricomi[a,b], C. Tuve[a,b]

INFN Sezione di Firenze[a], Università di Firenze[b], Firenze, Italy
G. Barbagli[a], V. Ciulli[a,b], C. Civinini[a], R. D'Alessandro[a,b], E. Focardi[a,b], E. Gallo[a], S. Gonzi[a,b], V. Gori[a,b,], P. Lenzi[a,b], M. Meschini[a], S. Paoletti[a], G. Sguazzoni[a], A. Tropiano[a,b]

INFN Laboratori Nazionali di Frascati, Frascati, Italy
L. Benussi, S. Bianco, F. Fabbri, D. Piccolo

INFN Sezione di Genova[a], Università di Genova[b], Genoa, Italy
R. Ferretti[a,b], F. Ferro[a], M. Lo Vetere[a,b], E. Robutti[a], S. Tosi[a,b]

INFN Sezione di Milano-Bicocca[a], Università di Milano-Bicocca[b], Milan, Italy
M. E. Dinardo[a,b], S. Fiorendi[a,b,], S. Gennai[a,2], R. Gerosa[a,b,2], A. Ghezzi[a,b], P. Govoni[a,b], M. T. Lucchini[a,b,2], S. Malvezzi[a], R. A. Manzoni[a,b], A. Martelli[a,b], B. Marzocchi[a,b,2], D. Menasce[a], L. Moroni[a], M. Paganoni[a,b], D. Pedrini[a], S. Ragazzi[a,b], N. Redaelli[a], T. Tabarelli de Fatis[a,b]

INFN Sezione di Napoli[a], Università di Napoli 'Federico II'[b], Università della Basilicata (Potenza)[c], Università G. Marconi (Roma)[d], Naples, Italy
S. Buontempo[a], N. Cavallo[a,c], S. Di Guida[a,d,2], F. Fabozzi[a,c], A. O. M. Iorio[a,b], L. Lista[a], S. Meola[a,d,2], M. Merola[a], P. Paolucci[a,2]

INFN Sezione di Padova[a], Università di Padova[b], Università di Trento (Trento)[c], Padua, Italy
P. Azzi[a], N. Bacchetta[a], D. Bisello[a,b], A. Branca[a,b], R. Carlin[a,b], P. Checchia[a], M. Dall'Osso[a,b], T. Dorigo[a], M. Galanti[a,b], U. Gasparini[a,b], P. Giubilato[a,b], F. Gonella[a], A. Gozzelino[a], K. Kanishchev[a,c], S. Lacaprara[a], M. Margoni[a,b], A. T. Meneguzzo[a,b], F. Montecassiano[a], J. Pazzini[a,b], N. Pozzobon[a,b], P. Ronchese[a,b], F. Simonetto[a,b], E. Torassa [a], M. Tosi[a,b], P. Zotto[a,b], A. Zucchetta[a,b], G. Zumerle[a,b]

INFN Sezione di Pavia[a], Università di Pavia[b], Pavia, Italy
M. Gabusi[a,b], S. P. Ratti[a,b], V. Re[a], C. Riccardi[a,b], P. Salvini[a], P. Vitulo[a,b]

INFN Sezione di Perugia[a], Università di Perugia[b], Perugia, Italy
M. Biasini[a,b], G. M. Bilei[a], D. Ciangottini[a,b,2], L. Fanò[a,b], P. Lariccia[a,b], G. Mantovani[a,b], M. Menichelli[a], A. Saha[a], A. Santocchia[a,b], A. Spiezia[a,b,2]

INFN Sezione di Pisa[a], Università di Pisa[b], Scuola Normale Superiore di Pisa[c], Pisa, Italy
K. Androsov[a,25], P. Azzurri[a], G. Bagliesi[a], J. Bernardini[a], T. Boccali[a], G. Broccolo[a,c], R. Castaldi[a], M. A. Ciocci[a,25], R. Dell'Orso[a], S. Donato[a,c,2], F. Fiori[a,c], L. Foà[a,c], A. Giassi[a], M. T. Grippo[a,25], F. Ligabue[a,c], T. Lomtadze[a], L. Martini[a,b], A. Messineo[a,b], C. S. Moon[a,26], F. Palla[a,2], A. Rizzi[a,b], A. Savoy-Navarro[a,27], A. T. Serban[a], P. Spagnolo[a], P. Squillacioti[a,25], R. Tenchini[a], G. Tonelli[a,b], A. Venturi[a], P. G. Verdini[a], C. Vernieri[a,c,]

INFN Sezione di Roma[a], Università di Roma[b], Rome, Italy
L. Barone[a,b], F. Cavallari[a], G. D'imperio[a,b], D. Del Re[a,b], M. Diemoz[a], C. Jorda[a], E. Longo[a,b], F. Margaroli[a,b], P. Meridiani[a], F. Micheli[a,b,2], S. Nourbakhsh[a,b], G. Organtini[a,b], R. Paramatti[a], S. Rahatlou[a,b], C. Rovelli[a], F. Santanastasio[a,b], L. Soffi[a,b,], P. Traczyk[a,b,2]

INFN Sezione di Torino[a], Università di Torino[b], Università del Piemonte Orientale (Novara)[c], Turin, Italy
N. Amapane[a,b], R. Arcidiacono[a,c], S. Argiro[a,b,], M. Arneodo[a,c], R. Bellan[a,b], C. Biino[a], N. Cartiglia[a], S. Casasso[a,b,2], M. Costa[a,b], A. Degano[a,b], N. Demaria[a], L. Finco[a,b,2], C. Mariotti[a], S. Maselli[a], E. Migliore[a,b], V. Monaco[a,b], M. Musich[a], M. M. Obertino[a,c,], G. Ortona[a,b], L. Pacher[a,b], N. Pastrone[a], M. Pelliccioni[a], G. L. Pinna Angioni[a,b], A. Potenza[a,b], A. Romero[a,b], M. Ruspa[a,c], R. Sacchi[a,b], A. Solano[a,b], A. Staiano[a], U. Tamponi[a]

INFN Sezione di Trieste[a], Università di Trieste[b], Trieste, Italy
S. Belforte[a], V. Candelise[a,b], M. Casarsa[a], F. Cossutti[a], G. Della Ricca[a,b], B. Gobbo[a], C. La Licata[a,b], M. Marone[a,b], A. Schizzi[a,b], T. Umer[a,b], A. Zanetti[a]

Kangwon National University, Chunchon, Korea
S. Chang, T. A. Kropivnitskaya, S. K. Nam

Kyungpook National University, Taegu, Korea
D. H. Kim, G. N. Kim, M. S. Kim, D. J. Kong, S. Lee, Y. D. Oh, H. Park, A. Sakharov, D. C. Son

Chonbuk National University, Chonju, Korea
T. J. Kim

Chonnam National University, Institute for Universe and Elementary Particles, Kwangju, Korea
J. Y. Kim, S. Song

Korea University, Seoul, Korea
S. Choi, D. Gyun, B. Hong, M. Jo, H. Kim, Y. Kim, B. Lee, K. S. Lee, S. K. Park, Y. Roh

Seoul National University, Seoul, Korea
H. D. Yoo

University of Seoul, Seoul, Korea
M. Choi, J. H. Kim, I. C. Park, G. Ryu, M. S. Ryu

Sungkyunkwan University, Suwon, Korea
Y. Choi, Y. K. Choi, J. Goh, D. Kim, E. Kwon, J. Lee, I. Yu

Vilnius University, Vilnius, Lithuania
A. Juodagalvis

National Centre for Particle Physics, Universiti Malaya, Kuala Lumpur, Malaysia
J. R. Komaragiri, M. A. B. Md Ali

Centro de Investigacion y de Estudios Avanzados del IPN, Mexico City, Mexico
E. Casimiro Linares, H. Castilla-Valdez, E. De La Cruz-Burelo, I. Heredia-de La Cruz[28], A. Hernandez-Almada, R. Lopez-Fernandez, A. Sanchez-Hernandez

Universidad Iberoamericana, Mexico City, Mexico
S. Carrillo Moreno, F. Vazquez Valencia

Benemerita Universidad Autonoma de Puebla, Puebla, Mexico
I. Pedraza, H. A. Salazar Ibarguen

Universidad Autónoma de San Luis Potosí, San Luis Potosí, Mexico
A. Morelos Pineda

University of Auckland, Auckland, New Zealand
D. Krofcheck

University of Canterbury, Christchurch, New Zealand
P. H. Butler, S. Reucroft

National Centre for Physics, Quaid-I-Azam University, Islamabad, Pakistan
A. Ahmad, M. Ahmad, Q. Hassan, H. R. Hoorani, W. A. Khan, T. Khurshid, M. Shoaib

National Centre for Nuclear Research, Swierk, Poland
H. Bialkowska, M. Bluj, B. Boimska, T. Frueboes, M. Górski, M. Kazana, K. Nawrocki, K. Romanowska-Rybinska, M. Szleper, P. Zalewski

Institute of Experimental Physics, Faculty of Physics, University of Warsaw, Warsaw, Poland
G. Brona, K. Bunkowski, M. Cwiok, W. Dominik, K. Doroba, A. Kalinowski, M. Konecki, J. Krolikowski, M. Misiura, M. Olszewski, W. Wolszczak

Laboratório de Instrumentação e Física Experimental de Partículas, Lisbon, Portugal
P. Bargassa, C. Beirão Da Cruz E Silva, P. Faccioli, P. G. Ferreira Parracho, M. Gallinaro, L. Lloret Iglesias, F. Nguyen, J. Rodrigues Antunes, J. Seixas, J. Varela, P. Vischia

Joint Institute for Nuclear Research, Dubna, Russia
S. Afanasiev, P. Bunin, M. Gavrilenko, I. Golutvin, I. Gorbunov, A. Kamenev, V. Karjavin, V. Konoplyanikov, A. Lanev, A. Malakhov, V. Matveev[29], P. Moisenz, V. Palichik, V. Perelygin, S. Shmatov, N. Skatchkov, V. Smirnov, A. Zarubin

Petersburg Nuclear Physics Institute, Gatchina, St. Petersburg, Russia
V. Golovtsov, Y. Ivanov, V. Kim[30], P. Levchenko, V. Murzin, V. Oreshkin, I. Smirnov, V. Sulimov, L. Uvarov, S. Vavilov, A. Vorobyev, An. Vorobyev

Institute for Nuclear Research, Moscow, Russia
Yu. Andreev, A. Dermenev, S. Gninenko, N. Golubev, M. Kirsanov, N. Krasnikov, A. Pashenkov, D. Tlisov, A. Toropin

Institute for Theoretical and Experimental Physics, Moscow, Russia
V. Epshteyn, V. Gavrilov, N. Lychkovskaya, V. Popov, I. Pozdnyakov, G. Safronov, S. Semenov, A. Spiridonov, V. Stolin, E. Vlasov, A. Zhokin

P. N. Lebedev Physical Institute, Moscow, Russia
V. Andreev, M. Azarkin[31], I. Dremin[31], M. Kirakosyan, A. Leonidov[31], G. Mesyats, S. V. Rusakov, A. Vinogradov

Skobeltsyn Institute of Nuclear Physics, Lomonosov Moscow State University, Moscow, Russia
A. Belyaev, E. Boos, A. Demiyanov, A. Ershov, A. Gribushin, O. Kodolova, V. Korotkikh, I. Lokhtin, S. Obraztsov, S. Petrushanko, V. Savrin, A. Snigirev, I. Vardanyan

State Research Center of Russian Federation, Institute for High Energy Physics, Protvino, Russia
I. Azhgirey, I. Bayshev, S. Bitioukov, V. Kachanov, A. Kalinin, D. Konstantinov, V. Krychkine, V. Petrov, R. Ryutin, A. Sobol, L. Tourtchanovitch, S. Troshin, N. Tyurin, A. Uzunian, A. Volkov

Faculty of Physics and Vinca Institute of Nuclear Sciences, University of Belgrade, Belgrade, Serbia
P. Adzic[32], M. Ekmedzic, J. Milosevic, V. Rekovic

Centro de Investigaciones Energéticas Medioambientales y Tecnológicas (CIEMAT), Madrid, Spain
J. Alcaraz Maestre, C. Battilana, E. Calvo, M. Cerrada, M. Chamizo Llatas, N. Colino, B. De La Cruz, A. Delgado Peris, D. Domínguez Vázquez, A. Escalante Del Valle, C. Fernandez Bedoya, J. P. Fernández Ramos, J. Flix, M. C. Fouz, P. Garcia-Abia, O. Gonzalez Lopez, S. Goy Lopez, J. M. Hernandez, M. I. Josa, E. Navarro De Martino, A. Pérez-Calero Yzquierdo, J. Puerta Pelayo, A. Quintario Olmeda, I. Redondo, L. Romero, M. S. Soares

Universidad Autónoma de Madrid, Madrid, Spain
C. Albajar, J. F. de Trocóniz, M. Missiroli, D. Moran

Universidad de Oviedo, Oviedo, Spain
H. Brun, J. Cuevas, J. Fernandez Menendez, S. Folgueras, I. Gonzalez Caballero

Instituto de Física de Cantabria (IFCA), CSIC-Universidad de Cantabria, Santander, Spain
J. A. Brochero Cifuentes, I. J. Cabrillo, A. Calderon, J. Duarte Campderros, M. Fernandez, G. Gomez, A. Graziano, A. Lopez Virto, J. Marco, R. Marco, C. Martinez Rivero, F. Matorras, F. J. Munoz Sanchez, J. Piedra Gomez, T. Rodrigo, A. Y. Rodríguez-Marrero, A. Ruiz-Jimeno, L. Scodellaro, I. Vila, R. Vilar Cortabitarte

CERN, European Organization for Nuclear Research, Geneva, Switzerland
D. Abbaneo, E. Auffray, G. Auzinger, M. Bachtis, P. Baillon, A. H. Ball, D. Barney, A. Benaglia, J. Bendavid, L. Benhabib, J. F. Benitez, C. Bernet[7], P. Bloch, A. Bocci, A. Bonato, O. Bondu, C. Botta, H. Breuker, T. Camporesi, G. Cerminara, S. Colafranceschi[33], M. D'Alfonso, D. d'Enterria, A. Dabrowski, A. David, F. De Guio, A. De Roeck, S. De Visscher, E. Di Marco, M. Dobson, M. Dordevic, B. Dorney, N. Dupont-Sagorin, A. Elliott-Peisert, G. Franzoni, W. Funk, D. Gigi, K. Gill, D. Giordano, M. Girone, F. Glege, R. Guida, S. Gundacker, M. Guthoff, J. Hammer, M. Hansen, P. Harris, J. Hegeman, V. Innocente, P. Janot, K. Kousouris, K. Krajczar, P. Lecoq, C. Lourenço, N. Magini, L. Malgeri, M. Mannelli, J. Marrouche, L. Masetti, F. Meijers, S. Mersi, E. Meschi, F. Moortgat, S. Morovic, M. Mulders, L. Orsini, L. Pape, E. Perez, L. Perrozzi, A. Petrilli, G. Petrucciani, A. Pfeiffer, M. Pimiä, D. Piparo, M. Plagge, A. Racz, G. Rolandi[34], M. Rovere, H. Sakulin, C. Schäfer, C. Schwick, A. Sharma, P. Siegrist, P. Silva, M. Simon, P. Sphicas[35], D. Spiga, J. Steggemann, B. Stieger, M. Stoye, Y. Takahashi, D. Treille, A. Tsirou, G. I. Veres[17], N. Wardle, H. K. Wöhri, H. Wollny, W. D. Zeuner

Paul Scherrer Institut, Villigen, Switzerland
W. Bertl, K. Deiters, W. Erdmann, R. Horisberger, Q. Ingram, H. C. Kaestli, D. Kotlinski, U. Langenegger, D. Renker, T. Rohe

Institute for Particle Physics, ETH Zurich, Zurich, Switzerland
F. Bachmair, L. Bäni, L. Bianchini, M. A. Buchmann, B. Casal, N. Chanon, G. Dissertori, M. Dittmar, M. Donegà, M. Dünser, P. Eller, C. Grab, D. Hits, J. Hoss, W. Lustermann, B. Mangano, A. C. Marini, M. Marionneau, P. Martinez Ruiz del Arbol, M. Masciovecchio, D. Meister, N. Mohr, P. Musella, C. Nägeli[37], F. Nessi-Tedaldi, F. Pandolfi, F. Pauss, M. Peruzzi, M. Quittnat, L. Rebane, M. Rossini, A. Starodumov[37], M. Takahashi, K. Theofilatos, R. Wallny, H. A. Weber

Universität Zürich, Zurich, Switzerland
C. Amsler[38], M. F. Canelli, V. Chiochia, A. De Cosa, A. Hinzmann, T. Hreus, B. Kilminster, C. Lange, B. Millan Mejias, J. Ngadiuba, D. Pinna, P. Robmann, F. J. Ronga, S. Taroni, M. Verzetti, Y. Yang

National Central University, Chung-Li, Taiwan
M. Cardaci, K. H. Chen, C. Ferro, C. M. Kuo, W. Lin, Y. J. Lu, R. Volpe, S. S. Yu

National Taiwan University (NTU), Taipei, Taiwan
P. Chang, Y. H. Chang, Y. W. Chang, Y. Chao, K. F. Chen, P. H. Chen, C. Dietz, U. Grundler, W.-S. Hou, K. Y. Kao, Y. F. Liu, R.-S. Lu, D. Majumder, E. Petrakou, Y. M. Tzeng, R. Wilken

Department of Physics, Faculty of Science, Chulalongkorn University, Bangkok, Thailand
B. Asavapibhop, G. Singh, N. Srimanobhas, N. Suwonjandee

Cukurova University, Adana, Turkey
A. Adiguzel, M. N. Bakirci[39], S. Cerci[40], C. Dozen, I. Dumanoglu, E. Eskut, S. Girgis, G. Gokbulut, E. Gurpinar, I. Hos, E. E. Kangal, A. Kayis Topaksu, G. Onengut[41], K. Ozdemir, S. Ozturk[39], A. Polatoz, D. Sunar Cerci[40], B. Tali[40], H. Topakli[39], M. Vergili

Physics Department, Middle East Technical University, Ankara, Turkey
I. V. Akin, B. Bilin, S. Bilmis, H. Gamsizkan[42], B. Isildak[43], G. Karapinar[44], K. Ocalan[45], S. Sekmen, U. E. Surat, M. Yalvac, M. Zeyrek

Bogazici University, Istanbul, Turkey
E. A. Albayrak[46], E. Gülmez, M. Kaya[47], O. Kaya[48], T. Yetkin[49]

Istanbul Technical University, Istanbul, Turkey
K. Cankocak, F. I. Vardarlı

National Scientific Center, Kharkov Institute of Physics and Technology, Kharkov, Ukraine
L. Levchuk, P. Sorokin

University of Bristol, Bristol, UK
J. J. Brooke, E. Clement, D. Cussans, H. Flacher, J. Goldstein, M. Grimes, G. P. Heath, H. F. Heath, J. Jacob, L. Kreczko, C. Lucas, Z. Meng, D. M. Newbold[50], S. Paramesvaran, A. Poll, T. Sakuma, S. Senkin, V. J. Smith, T. Williams

Rutherford Appleton Laboratory, Didcot, UK
A. Belyaev[51], C. Brew, R. M. Brown, D. J. A. Cockerill, J. A. Coughlan, K. Harder, S. Harper, E. Olaiya, D. Petyt, C. H. Shepherd-Themistocleous, A. Thea, I. R. Tomalin, W. J. Womersley, S. D. Worm

Imperial College, London, UK
M. Baber, R. Bainbridge, O. Buchmuller, D. Burton, D. Colling, N. Cripps, P. Dauncey, G. Davies, M. Della Negra, P. Dunne, W. Ferguson, J. Fulcher, D. Futyan, G. Hall, G. Iles, M. Jarvis, G. Karapostoli, M. Kenzie, R. Lane, R. Lucas[50], L. Lyons, A.-M. Magnan, S. Malik, B. Mathias, J. Nash, A. Nikitenko[37], J. Pela, M. Pesaresi, K. Petridis, D. M. Raymond, S. Rogerson, A. Rose, C. Seez, P. Sharp[†], A. Tapper, M. Vazquez Acosta, T. Virdee, S. C. Zenz

Brunel University, Uxbridge, UK
J. E. Cole, P. R. Hobson, A. Khan, P. Kyberd, D. Leggat, D. Leslie, I. D. Reid, P. Symonds, L. Teodorescu, M. Turner

Baylor University, Waco, USA
J. Dittmann, K. Hatakeyama, A. Kasmi, H. Liu, T. Scarborough

The University of Alabama, Tuscaloosa, USA
O. Charaf, S. I. Cooper, C. Henderson, P. Rumerio

Boston University, Boston, USA
A. Avetisyan, T. Bose, C. Fantasia, P. Lawson, C. Richardson, J. Rohlf, J. St. John, L. Sulak

Brown University, Providence, USA
J. Alimena, E. Berry, S. Bhattacharya, G. Christopher, D. Cutts, Z. Demiragli, N. Dhingra, A. Ferapontov, A. Garabedian, U. Heintz, G. Kukartsev, E. Laird, G. Landsberg, M. Luk, M. Narain, M. Segala, T. Sinthuprasith, T. Speer, J. Swanson

University of California, Davis, USA
R. Breedon, G. Breto, M. Calderon De La Barca Sanchez, S. Chauhan, M. Chertok, J. Conway, R. Conway, P. T. Cox, R. Erbacher, M. Gardner, W. Ko, R. Lander, M. Mulhearn, D. Pellett, J. Pilot, F. Ricci-Tam, S. Shalhout, J. Smith, M. Squires, D. Stolp, M. Tripathi, S. Wilbur, R. Yohay

University of California, Los Angeles, USA
R. Cousins, P. Everaerts, C. Farrell, J. Hauser, M. Ignatenko, G. Rakness, E. Takasugi, V. Valuev, M. Weber

University of California, Riverside, Riverside, USA
K. Burt, R. Clare, J. Ellison, J. W. Gary, G. Hanson, J. Heilman, M. Ivova Rikova, P. Jandir, E. Kennedy, F. Lacroix, O. R. Long, A. Luthra, M. Malberti, M. Olmedo Negrete, A. Shrinivas, S. Sumowidagdo, S. Wimpenny

University of California, San Diego, La Jolla, USA
J. G. Branson, G. B. Cerati, S. Cittolin, R. T. D'Agnolo, A. Holzner, R. Kelley, D. Klein, J. Letts, I. Macneill, D. Olivito, S. Padhi, C. Palmer, M. Pieri, M. Sani, V. Sharma, S. Simon, M. Tadel, Y. Tu, A. Vartak, C. Welke, F. Würthwein, A. Yagil

University of California, Santa Barbara, Santa Barbara, USA
D. Barge, J. Bradmiller-Feld, C. Campagnari, T. Danielson, A. Dishaw, V. Dutta, K. Flowers, M. Franco Sevilla, P. Geffert, C. George, F. Golf, L. Gouskos, J. Incandela, C. Justus, N. Mccoll, J. Richman, D. Stuart, W. To, C. West, J. Yoo

California Institute of Technology, Pasadena, USA
A. Apresyan, A. Bornheim, J. Bunn, Y. Chen, J. Duarte, A. Mott, H. B. Newman, C. Pena, M. Pierini, M. Spiropulu, J. R. Vlimant, R. Wilkinson, S. Xie, R. Y. Zhu

Carnegie Mellon University, Pittsburgh, USA
V. Azzolini, A. Calamba, B. Carlson, T. Ferguson, Y. Iiyama, M. Paulini, J. Russ, H. Vogel, I. Vorobiev

University of Colorado at Boulder, Boulder, USA
J. P. Cumalat, W. T. Ford, A. Gaz, M. Krohn, E. Luiggi Lopez, U. Nauenberg, J. G. Smith, K. Stenson, K. A. Ulmer, S. R. Wagner

Cornell University, Ithaca, USA
J. Alexander, A. Chatterjee, J. Chaves, J. Chu, S. Dittmer, N. Eggert, N. Mirman, G. Nicolas Kaufman, J. R. Patterson, A. Ryd, E. Salvati, L. Skinnari, W. Sun, W. D. Teo, J. Thom, J. Thompson, J. Tucker, Y. Weng, L. Winstrom, P. Wittich

Fairfield University, Fairfield, USA
D. Winn

Fermi National Accelerator Laboratory, Batavia, USA
S. Abdullin, M. Albrow, J. Anderson, G. Apollinari, L. A. T. Bauerdick, A. Beretvas, J. Berryhill, P. C. Bhat, G. Bolla, K. Burkett, J. N. Butler, H. W. K. Cheung, F. Chlebana, S. Cihangir, V. D. Elvira, I. Fisk, J. Freeman, Y. Gao, E. Gottschalk, L. Gray, D. Green, S. Grünendahl, O. Gutsche, J. Hanlon, D. Hare, R. M. Harris, J. Hirschauer, B. Hooberman, S. Jindariani, M. Johnson, U. Joshi, K. Kaadze, B. Klima, B. Kreis, S. Kwan, J. Linacre, D. Lincoln, R. Lipton, T. Liu, J. Lykken, K. Maeshima, J. M. Marraffino, V. I. Martinez Outschoorn, S. Maruyama, D. Mason, P. McBride, P. Merkel, K. Mishra, S. Mrenna, S. Nahn, C. Newman-Holmes, V. O'Dell, O. Prokofyev, E. Sexton-Kennedy, S. Sharma, A. Soha, W. J. Spalding, L. Spiegel, L. Taylor, S. Tkaczyk, N. V. Tran, L. Uplegger, E. W. Vaandering, R. Vidal, A. Whitbeck, J. Whitmore, F. Yang

University of Florida, Gainesville, USA
D. Acosta, P. Avery, P. Bortignon, D. Bourilkov, M. Carver, D. Curry, S. Das, M. De Gruttola, G. P. Di Giovanni, R. D. Field, M. Fisher, I. K. Furic, J. Hugon, J. Konigsberg, A. Korytov, T. Kypreos, J. F. Low, K. Matchev, H. Mei, P. Milenovic[52], G. Mitselmakher, L. Muniz, A. Rinkevicius, L. Shchutska, M. Snowball, D. Sperka, J. Yelton, M. Zakaria

Florida International University, Miami, USA
S. Hewamanage, S. Linn, P. Markowitz, G. Martinez, J. L. Rodriguez

Florida State University, Tallahassee, USA
T. Adams, A. Askew, J. Bochenek, B. Diamond, J. Haas, S. Hagopian, V. Hagopian, K. F. Johnson, H. Prosper, V. Veeraraghavan, M. Weinberg

Florida Institute of Technology, Melbourne, USA
M. M. Baarmand, M. Hohlmann, H. Kalakhety, F. Yumiceva

University of Illinois at Chicago (UIC), Chicago, USA
M. R. Adams, L. Apanasevich, D. Berry, R. R. Betts, I. Bucinskaite, R. Cavanaugh, O. Evdokimov, L. Gauthier, C. E. Gerber, D. J. Hofman, P. Kurt, D. H. Moon, C. O'Brien, I. D. Sandoval Gonzalez, C. Silkworth, P. Turner, N. Varelas

The University of Iowa, Iowa City, USA
B. Bilki[53], W. Clarida, K. Dilsiz, M. Haytmyradov, J.-P. Merlo, H. Mermerkaya[54], A. Mestvirishvili, A. Moeller, J. Nachtman, H. Ogul, Y. Onel, F. Ozok[46], A. Penzo, R. Rahmat, S. Sen, P. Tan, E. Tiras, J. Wetzel, K. Yi

Johns Hopkins University, Baltimore, USA
B. A. Barnett, B. Blumenfeld, S. Bolognesi, D. Fehling, A. V. Gritsan, P. Maksimovic, C. Martin, M. Swartz

The University of Kansas, Lawrence, USA
P. Baringer, A. Bean, G. Benelli, C. Bruner, R. P. KennyIII, M. Malek, M. Murray, D. Noonan, S. Sanders, J. Sekaric, R. Stringer, Q. Wang, J. S. Wood

Kansas State University, Manhattan, USA
I. Chakaberia, A. Ivanov, S. Khalil, M. Makouski, Y. Maravin, L. K. Saini, N. Skhirtladze, I. Svintradze

Lawrence Livermore National Laboratory, Livermore, USA
J. Gronberg, D. Lange, F. Rebassoo, D. Wright

University of Maryland, College Park, USA
A. Baden, A. Belloni, B. Calvert, S. C. Eno, J. A. Gomez, N. J. Hadley, R. G. Kellogg, T. Kolberg, Y. Lu, A. C. Mignerey, K. Pedro, A. Skuja, M. B. Tonjes, S. C. Tonwar

Massachusetts Institute of Technology, Cambridge, USA
A. Apyan, R. Barbieri, G. Bauer, W. Busza, I. A. Cali, M. Chan, L. Di Matteo, G. Gomez Ceballos, M. Goncharov, D. Gulhan, M. Klute, Y. S. Lai, Y.-J. Lee, A. Levin, P. D. Luckey, T. Ma, C. Paus, D. Ralph, C. Roland, G. Roland, G. S. F. Stephans, F. Stöckli, K. Sumorok, D. Velicanu, J. Veverka, B. Wyslouch, M. Yang, M. Zanetti, V. Zhukova

University of Minnesota, Minneapolis, USA
B. Dahmes, A. Gude, S. C. Kao, K. Klapoetke, Y. Kubota, J. Mans, N. Pastika, R. Rusack, A. Singovsky, N. Tambe, J. Turkewitz

University of Mississippi, Oxford, USA
J. G. Acosta, S. Oliveros

University of Nebraska-Lincoln, Lincoln, USA
E. Avdeeva, K. Bloom, S. Bose, D. R. Claes, A. Dominguez, R. Gonzalez Suarez, J. Keller, D. Knowlton, I. Kravchenko, J. Lazo-Flores, F. Meier, F. Ratnikov, G. R. Snow, M. Zvada

State University of New York at Buffalo, Buffalo, USA
J. Dolen, A. Godshalk, I. Iashvili, A. Kharchilava, A. Kumar, S. Rappoccio

Northeastern University, Boston, USA
G. Alverson, E. Barberis, D. Baumgartel, M. Chasco, A. Massironi, D. M. Morse, D. Nash, T. Orimoto, D. Trocino, R. J. Wang, D. Wood, J. Zhang

Northwestern University, Evanston, USA
K. A. Hahn, A. Kubik, N. Mucia, N. Odell, B. Pollack, A. Pozdnyakov, M. Schmitt, S. Stoynev, K. Sung, M. Velasco, S. Won

University of Notre Dame, Notre Dame, USA
A. Brinkerhoff, K. M. Chan, A. Drozdetskiy, M. Hildreth, C. Jessop, D. J. Karmgard, N. Kellams, K. Lannon, S. Lynch, N. Marinelli, Y. Musienko[29], T. Pearson, M. Planer, R. Ruchti, G. Smith, N. Valls, M. Wayne, M. Wolf, A. Woodard

The Ohio State University, Columbus, USA
L. Antonelli, J. Brinson, B. Bylsma, L. S. Durkin, S. Flowers, A. Hart, C. Hill, R. Hughes, K. Kotov, T. Y. Ling, W. Luo, D. Puigh, M. Rodenburg, B. L. Winer, H. Wolfe, H. W. Wulsin

Princeton University, Princeton, USA
O. Driga, P. Elmer, J. Hardenbrook, P. Hebda, A. Hunt, S. A. Koay, P. Lujan, D. Marlow, T. Medvedeva, M. Mooney, J. Olsen, P. Piroué, X. Quan, H. Saka, D. Stickland[2], C. Tully, J. S. Werner, A. Zuranski

University of Puerto Rico, Mayaguez, USA
E. Brownson, S. Malik, H. Mendez, J. E. Ramirez Vargas

Purdue University, West Lafayette, USA
V. E. Barnes, D. Benedetti, D. Bortoletto, M. De Mattia, L. Gutay, Z. Hu, M. K. Jha, M. Jones, K. Jung, M. Kress, N. Leonardo, D. H. Miller, N. Neumeister, B. C. Radburn-Smith, X. Shi, I. Shipsey, D. Silvers, A. Svyatkovskiy, F. Wang, W. Xie, L. Xu, J. Zablocki

Purdue University Calumet, Hammond, USA
N. Parashar, J. Stupak

Rice University, Houston, USA
A. Adair, B. Akgun, K. M. Ecklund, F. J. M. Geurts, W. Li, B. Michlin, B. P. Padley, R. Redjimi, J. Roberts, J. Zabel

University of Rochester, Rochester, USA
B. Betchart, A. Bodek, R. Covarelli, P. de Barbaro, R. Demina, Y. Eshaq, T. Ferbel, A. Garcia-Bellido, P. Goldenzweig, J. Han, A. Harel, A. Khukhunaishvili, S. Korjenevski, G. Petrillo, D. Vishnevskiy

The Rockefeller University, New York, USA
R. Ciesielski, L. Demortier, K. Goulianos, C. Mesropian

Rutgers, The State University of New Jersey, Piscataway, USA
S. Arora, A. Barker, J. P. Chou, C. Contreras-Campana, E. Contreras-Campana, D. Duggan, D. Ferencek, Y. Gershtein, R. Gray, E. Halkiadakis, D. Hidas, S. Kaplan, A. Lath, S. Panwalkar, M. Park, R. Patel, S. Salur, S. Schnetzer, S. Somalwar, R. Stone, S. Thomas, P. Thomassen, M. Walker

University of Tennessee, Knoxville, USA
K. Rose, S. Spanier, A. York

Texas A&M University, College Station, USA
O. Bouhali[55], A. Castaneda Hernandez, R. Eusebi, W. Flanagan, J. Gilmore, T. Kamon[56], V. Khotilovich, V. Krutelyov, R. Montalvo, I. Osipenkov, Y. Pakhotin, A. Perloff, J. Roe, A. Rose, A. Safonov, I. Suarez, A. Tatarinov

Texas Tech University, Lubbock, USA
N. Akchurin, C. Cowden, J. Damgov, C. Dragoiu, P. R. Dudero, J. Faulkner, K. Kovitanggoon, S. Kunori, S. W. Lee, T. Libeiro, I. Volobouev

Vanderbilt University, Nashville, USA
E. Appelt, A. G. Delannoy, S. Greene, A. Gurrola, W. Johns, C. Maguire, Y. Mao, A. Melo, M. Sharma, P. Sheldon, B. Snook, S. Tuo, J. Velkovska

University of Virginia, Charlottesville, USA
M. W. Arenton, S. Boutle, B. Cox, B. Francis, J. Goodell, R. Hirosky, A. Ledovskoy, H. Li, C. Lin, C. Neu, J. Wood

Wayne State University, Detroit, USA
C. Clarke, R. Harr, P. E. Karchin, C. Kottachchi Kankanamge Don, P. Lamichhane, J. Sturdy

University of Wisconsin, Madison, USA
D. A. Belknap, D. Carlsmith, M. Cepeda, S. Dasu, L. Dodd, S. Duric, E. Friis, R. Hall-Wilton, M. Herndon, A. Hervé, P. Klabbers, A. Lanaro, C. Lazaridis, A. Levine, R. Loveless, A. Mohapatra, I. Ojalvo, T. Perry, G. A. Pierro, G. Polese, I. Ross, T. Sarangi, A. Savin, W. H. Smith, D. Taylor, C. Vuosalo, N. Woods

† **Deceased**

1: Also at Vienna University of Technology, Vienna, Austria
2: Also at CERN, European Organization for Nuclear Research, Geneva, Switzerland

3: Also at Institut Pluridisciplinaire Hubert Curien, Université de Strasbourg, Université de Haute Alsace Mulhouse, CNRS/IN2P3, Strasbourg, France
4: Also at National Institute of Chemical Physics and Biophysics, Tallinn, Estonia
5: Also at Skobeltsyn Institute of Nuclear Physics, Lomonosov Moscow State University, Moscow, Russia
6: Also at Universidade Estadual de Campinas, Campinas, Brazil
7: Also at Laboratoire Leprince-Ringuet, Ecole Polytechnique, IN2P3-CNRS, Palaiseau, France
8: Also at Joint Institute for Nuclear Research, Dubna, Russia
9: Also at Suez University, Suez, Egypt
10: Also at Cairo University, Cairo, Egypt
11: Also at Fayoum University, El-Fayoum, Egypt
12: Also at British University in Egypt, Cairo, Egypt
13: Now at Ain Shams University, Cairo, Egypt
14: Also at Université de Haute Alsace, Mulhouse, France
15: Also at Brandenburg University of Technology, Cottbus, Germany
16: Also at Institute of Nuclear Research ATOMKI, Debrecen, Hungary
17: Also at Eötvös Loránd University, Budapest, Hungary
18: Also at University of Debrecen, Debrecen, Hungary
19: Also at University of Visva-Bharati, Santiniketan, India
20: Now at King Abdulaziz University, Jeddah, Saudi Arabia
21: Also at University of Ruhuna, Matara, Sri Lanka
22: Also at Isfahan University of Technology, Isfahan, Iran
23: Also at University of Tehran, Department of Engineering Science, Tehran, Iran
24: Also at Plasma Physics Research Center, Science and Research Branch, Islamic Azad University, Tehran, Iran
25: Also at Università degli Studi di Siena, Siena, Italy
26: Also at Centre National de la Recherche Scientifique (CNRS)-IN2P3, Paris, France
27: Also at Purdue University, West Lafayette, USA
28: Also at Universidad Michoacana de San Nicolas de Hidalgo, Morelia, Mexico
29: Also at Institute for Nuclear Research, Moscow, Russia
30: Also at St. Petersburg State Polytechnical University, St. Petersburg, Russia
31: Also at National Research Nuclear University 'Moscow Engineering Physics Institute' (MEPhI), Moscow, Russia
32: Also at Faculty of Physics, University of Belgrade, Belgrade, Serbia
33: Also at Facoltà Ingegneria, Università di Roma, Rome, Italy
34: Also at Scuola Normale e Sezione dell'INFN, Pisa, Italy
35: Also at University of Athens, Athens, Greece
36: Also at Paul Scherrer Institut, Villigen, Switzerland
37: Also at Institute for Theoretical and Experimental Physics, Moscow, Russia
38: Also at Albert Einstein Center for Fundamental Physics, Bern, Switzerland
39: Also at Gaziosmanpasa University, Tokat, Turkey
40: Also at Adiyaman University, Adiyaman, Turkey
41: Also at Cag University, Mersin, Turkey
42: Also at Anadolu University, Eskisehir, Turkey
43: Also at Ozyegin University, Istanbul, Turkey
44: Also at Izmir Institute of Technology, Izmir, Turkey
45: Also at Necmettin Erbakan University, Konya, Turkey
46: Also at Mimar Sinan University, Istanbul, Istanbul, Turkey
47: Also at Marmara University, Istanbul, Turkey
48: Also at Kafkas University, Kars, Turkey
49: Also at Yildiz Technical University, Istanbul, Turkey
50: Also at Rutherford Appleton Laboratory, Didcot, UK
51: Also at School of Physics and Astronomy, University of Southampton, Southampton, UK
52: Also at University of Belgrade, Faculty of Physics and Vinca Institute of Nuclear Sciences, Belgrade, Serbia
53: Also at Argonne National Laboratory, Argonne, USA

54: Also at Erzincan University, Erzincan, Turkey
55: Also at Texas A&M University at Qatar, Doha, Qatar
56: Also at Kyungpook National University, Taegu, Korea